THEORETICAL STUDY ON GENERATING LUMINOUS AND CONTROLLED FIGURES BY SPONTANEOUS EMISSION

Relatore:
Prof. Mauro Villa

Presentata da:
Stefano Bianchi

Abstract

La presente tesi si pone come obiettivo lo studio di meccanismi in grado di generare figure luminose nello spazio. Il metodo proposto è quello di riuscire a illuminare un piccolo punto nello spazio e di muoverlo ad una velocità tale da dare l'illusione di osservare un immagine fissa. Tale punto si assume che possa essere replicato più volte, in modo tale da costruire immagini più complesse grazie alla combinazione degli effetti.

Il principio fisico a supporto dell'idea è stato trovato nei fenomeni di emissione spontanea, quindi in quei processi che vedono un atomo passare spontaneamente da uno stato elettronico eccitato a uno ad energia minore, liberando fotoni. Si sceglie di utilizzare uno schema di transizioni a quattro livelli energetici e di studiare la dinamica delle popolazioni di ciascun livello in funzione del tempo; la scelta di uno schema a quattro livelli è suggerita dalla possibilità di ottenere un emissione di fotoni "visibili", quindi con frequenza appartenente allo spettro visibile, a seguito di un eccitazione da parte di due laser "non visibili", in particolare infrarossi. Questa configurazione è particolarmente efficace se si considerano atomi con un unico elettrone di valenza.

Inoltre, si vuole ricercare un elemento chimico che rispetti esattamente le condizioni richieste per eseguire le transizioni specificate; tra i vari elementi possibili è stato scelto il rubidio in stato gassoso, con i relativi livelli energetici da utilizzare.

Contents

Introduction

There's one cool gadget, besides lightsabers, that Star Wars franchise depicted very carefully: 3D holograms. Now, as it usually happens in science fiction movies, they don't explain very accurately how those devices are made, or what is the physical principle behind them; we just have to invent it ourselves. It is therefore important to identify the physical phenomena that could help us reproduce a similar result and comprehend it deeply in order to being able to utilize it properly. Now, the standard quality of a 3D hologram that has been established in the collective imagination is way far beyond any possible result we can obtain by now; the aim of this study is to see if it's actually possible to create the conditions required for a 3D hologram and then try to give an analytical model that describes it.

The content of this thesis is as follows: In the first chapter, we describe in general what are the light production processes, focusing especially in *photoluminescence* phenomena which are *fluorescence* and *phosphorescence*. In addition, we show some concrete applications of those two processes, both in science and in everyday entertainment. Then we report some of the latest studies in 3D hologram field, which are carried out by relatively small companies; in order to generate a luminous image, some of them use scattering, others high intensity lasers that cause air ionization, which then emits light and noise (plasma).

In chapter two, we give an introduction to the theory needed to understand our project; the main topics are the *atomic model*, with the fundamental steps that improved it over time, and the theory of *spontaneous and stimulated emissions*, which is of primary interest for the study.

In the last chapter we introduce the mathematical modeling of a four level transition scheme, that is the one that allows us to generate visible light using non-visible lasers. As we will see during the study, we had to make significant approximations in order to obtain an analytical solution to the problem; with a good amount of well-aimed experimental data it would be easier to make a better mathematical model of the system, that we leave for future developments of this subject.

Chapter 1

Luminous experiments and technologies

We shall approach our study on *generating luminous figures* with a quick look at what has already been done in the last centuries and what we could use to take inspiration from. Countless studies have been carried out on inspecting luminescence phenomena, especially in the last century. In this chapter, we will briefly introduce the methods used to generate light; in particular, our attention will be focused on *fluorescence* and *phosphorescence*, which goes under the category of *photoluminescence*. After a simple introduction on the processes that can generate electromagnetic radiation, we will take a look at the historical background, showing the main known discoveries and retracing the major studies made by Stokes, Jean Perrin and Francis Perrin. Then we will properly define the differences between *fluorescence* and *phosphorescence*, which can be explained only by using quantum mechanics, and we will see some examples of end-uses in science and entertainment. For the sake of completeness, at the end of this introduction we will list some of the current techniques and prototypes to create what is roughly called a "hologram".

Before we begin, let's report a funny comment that gives a proper idea of the amount of work that has been done in this field (like in any other field of science). Right in the introduction of his paper entitled *"Uses of Fluorescence in Biophysics: some recent developments"*, Gregorio Weber, one of the most important scientist in the field of fluorescence, said: *"The use of fluorescence emission ... has undergone rapid development in the past fifteen years so that it is already next to impossible for any one person to keep up with the vast amount of information presented"*; we'll be sure to always keep those words in mind.

1.1   Light production processes

First of all, we have to clarify that a general body has several ways to emit light, depending on its physical and chemical properties. There are indeed many physical phenomena identified as *luminescence* which differ from the others by the chemical reaction involved and the duration of the process; here we have a list of the main subcategories of luminescence[1]:

- *Chemiluminescence*: A material emits electromagnetic radiation as the result of a chemical reaction; this involves even light emitted by certain materials at elevated temperatures.

- *Crystalloluminescence*: A materials may emits electromagnetic radiation during crystal growth and destruction[2].

- *Electroluminescence*: A material traversed by a current or a strong electric field may generate optic and electromagnetic phenomena; this doesn't involve emission resulting from heat.

- *Mechanoluminescence*: A material subject to a mechanical action, such as increase pressure or traction, may emits electromagnetic radiation.

- *Photoluminescence*: This phenomenon is the light emission from any form of matter after the interaction with electromagnetic radiation (*photons*); it is in turn divided in two physical phenomena: *fluorescence* and *phosphorescence*. It is of primary interest for our theoretical study.

- *Radioluminescence*: A material bombarded with ionizing radiation, such as alpha particles, beta particles, or gamma rays may emits electromagnetic radiation.

- *Thermoluminescence*: A material exposed to electromagnetic radiation (or even ionizing radiation) and heated up by absorbing its energy may re-emit it; this process can continue even once the source of radiation is switched off.

Instead of using the word *"light"*, we have carefully used the term *"electromagnetic radiation"*, because many of this phenomena might emit radiation outside the visible spectrum, which can be misunderstood. We will not describe all the points listed above, but we will fully tackle the *Photoluminescence* and its end-uses.

1.1.1   Phosphorescence and fluorescence

It has already been said that photoluminescence is divided in two different subsections, which are fluorescence and phosphorescence. The term *phosphorescence* comes from the Greek ($\phi\omega\varsigma = light$ and $\phi o\varrho\varepsilon\iota\nu = to\ bear$). In fact, phosphor literally means

"which bears light". The term phosphor has indeed been assigned since the Middle Ages to materials that glow in the dark after exposure to light[3]. Materials that exhibit this property were known long time ago; the images displayed in Figure 1.1 and Figure 1.2 show the typical behavior of a phosphorescent material, which emits light for some time after exposure, with a typical decrease in intensity as a function of time.
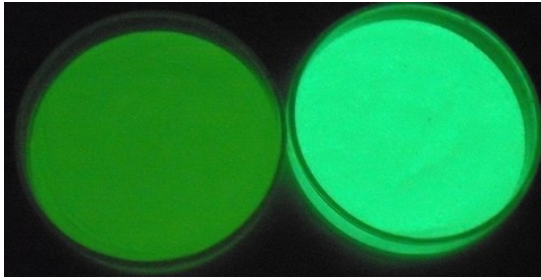
Figure 1.1: Light emitted by pigments of zinc sulfide ZnS (left) and strontium aluminate $SrAl_2O_4$ (right) 1 minute after light exposure.
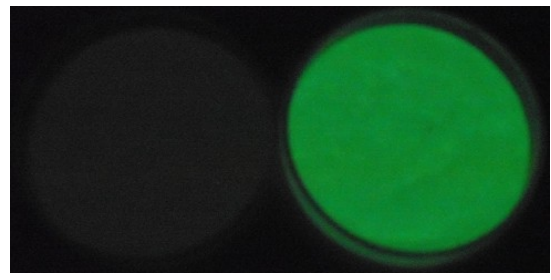
Figure 1.2: Light emitted by pigments of zinc sulfide ZnS (left) and strontium aluminate $SrAl_2O_4$ (right) 4 minutes after light exposure.

One of the most famous material with phosphorescence properties (but not the earliest known) was the *Bolognian phosphorus* (impure barium sulfide), discovered by Vincenzo Cascariolo (1571-1624) in the 1602. Later, the same name phosphor was assigned to the element phosphorus isolated by the German merchant and alchemist Hennig Brand (1630-1710) in 1677 because, when exposed to air, it burns and releases glowing vapors. The light emitted due to this process is in this case chemiluminescence, not photolumines-cence; the species that emit light are excited by the energy provided by the combustion reaction and not by the absorption of a photon[4]. The history of the term *fluorescence* is more recent and straight forward; it was coined by the mathematical and physician George Stokes in one of his studies of refrangibility of light in the middle of the 19th century. In his first paper, Stokes called the observed phenomenon *dispersive reflexion*, but in a footnote he wrote *"I confess I do not like this term. I am almost inclined to coin a word, and call the appearance fluorescence, from fluorspar, as analogous term opalescence is derived from the name of a mineral."*[5].

For a long time after Stokes' studies and papers, the distinction between fluorescence and phosphorescence was based on the duration of emission after the end of the interaction with the radiation source: fluorescence was considered as an emission of light that disap-pears very quickly ($\sim 10^{-8}s$) when ending the excitation, whereas in phosphorescence,

the emitted light persists for a variable time after the end of the excitation, that can be seconds, days or even years[4]. However this empirical distinction was insufficient in order to rigorously define the two phenomena. A proper separation between the two arrived after the advent of quantum theory and with that the better understanding of atomic orbitals. Two of the main scientists who dedicated about a decade each to the study of luminescence were Jean Perrin (1870-1942) and Francis Perrin (1901-1992).

Jean Perrin was one of the first to apply the ideas of quantum theory to the absorption and emission of radiation by molecules. In particular, he even presented a molecular energy diagram with transitions between states, which was probably the first time in history[6][7]. His son Francis Perrin continued and extended his father's studies, working in his laboratory from 1924, with many and important personal contributions[8][9]. In that period, another important scientist devoted to luminescence theory was the Polish physics Aleksander Jablonski (1898-1980), to whom is attributed the *Jablonski diagram*. The history of the diagram has been the subject of a recent and thorough investigation[10]. The Jablonski diagram shows that the fluorescent state of a molecular entity is the lowest excited state from which the transition to the ground state is allowed, whereas the phosphorescent state is a metastable state below the fluorescent state, which is reached by radiationless transition. From their studies and the introduction of the Jablonski diagram is now possible to properly distinguish the phenomena, like shown in Figure 1.3.

Both phosphorescence and fluorescence are generated by spontaneous emission of electromagnetic radiation. After the exposure to source of light, the molecules (or atoms) adsorb energy and make a transition from the ground state $E_{0,0}$ to an excited one $E_{1,i}$, where we used $E_{n,i}$ to indicate all the energy levels of our system, the main ones denoted with n and the ones with minor energy impact with i; the previous levels are only used as an example. We see from the Figure 1.3 that the difference between fluorescence and phosphorescence are due to the emission from a *singlet state* and a *triplet state* respectively. A singlet state is a quantum mechanic system in which the overall spin quantum number vanishes, $S = 0$. This means that all the electrons in a singlet state are paired. On the contrary, a triplet state (sometimes called *metastable*) is a quantum mechanics system in which the total spin is $S = 1$, therefore we have three allowed values of the third component of the spin $m_s = -1, 0, 1$. This specific issue will be considered in detail later on.

With this deeper knowledge of what happens at the atomic level, it is possible to give the modern definition of the two phenomena using spin multiplicity; we consider *fluorescence* when a molecule (or atom) transit from singlet state $E_{1,i}$ directly to the ground state and we have *phosphorescence* when the decay happens with an intermediate triplet state $E_{1,j}$, through a process called *intersystem crossing*. This process is enhanced if the vibrational levels of the two excited state are very close, since little energy must be exchanged. We know from quantum mechanics that transitions from ground
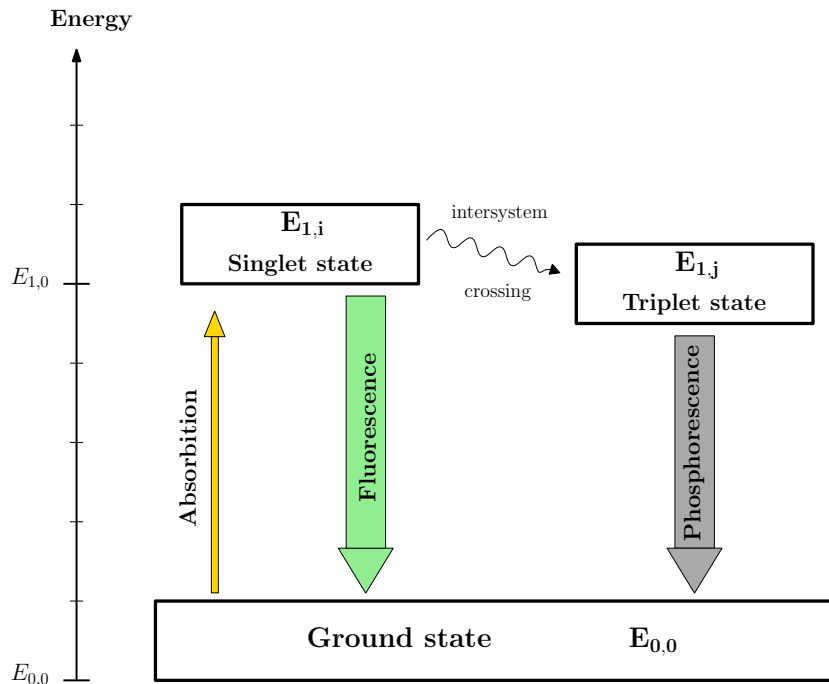
Figure 1.3: The Jablonski diagram of the necessary steps to generate fluorescence and phosphorescence phenomena.

state to an excited triplet state are forbidden. This fact implies that some others techniques are required to get our system in to the excited triplet state. Transitions between excited singlets and triplets depends on the energy gap and have a vanishing probability for most of the materials; but for some materials the energies are so close that transitions do occur. In these cases the transitions are called intersystem crossing and can happen just by thermal motion. When a system is in a triplet state it can either fall to the ground state (generating phosphorescence) or go back to the singlet one by energy exchange; every state is represented in Figure 1.4. Finally, we also
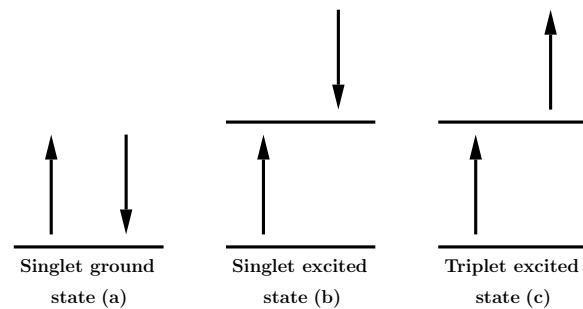
Figure 1.4: Schematization of singlet and triplet energy levels. The arrows represent the spin orientation of the electrons, the horizontal lines the levels.

understand why the duration of the two processes is different; quantum theory shows us that every transition has its probability to occur and with that a certain rate. It is more likely for a system to decay from a singlet state to the ground rather than a triplet; that's even the reason why the excited triplet state is called metastable as it is definitely more

stable than the others. There are different methods that quantify photoluminescence lifetime; the easiest approach to the problem is by set the following differential equation:

$$\dot{N}(t) = -\frac{1}{\tau(t)} N(t) \ , \tag{1.1}$$

where $N(t)$ is the time dependent number of excited molecules and $\tau(t)$ is the decay time of the system. If $\tau(t) = \tau_0$ is constant, we have the exponential solution:

$$N(t) = N_0 \, e^{-\frac{t}{\tau_0}} + N_1 \ , \tag{1.2}$$

with N_0 the number of the initially excited molecules and a constant N_1 that can be omitted. For example, the decay of protein fluorescence is usually described by a *multiexponential model*, therefore an arithmetic sum of exponents characterized by their specific parameters. Now, recent studies have shown that experimental data are better explained by a *power-like function*[11], which is:

$$N(t) = \frac{2-q}{\tau_0} \left[1 - (1-q)\frac{t}{\tau_0} \right]^{\frac{1}{(1-q)}} \ . \tag{1.3}$$

In this case, τ_0 represent the mean value of lifetime distribution and q is called parameter of heterogeneity, which describe the relative variance of fluctuations of $\gamma \equiv \frac{1}{\tau}$ around $\gamma \equiv \frac{1}{\tau_0}$ [11]:

$$q = 1 + \frac{\langle (\gamma - \langle \gamma \rangle)^2 \rangle}{\langle \gamma \rangle^2} = 1 + \frac{2}{N} \ . \tag{1.4}$$

The mean decay time $\langle t_d \rangle$ is obtained from the integration of equation (1.3), which gives:

$$\langle t_d \rangle = \frac{\tau_0}{3 - 2q} \ . \tag{1.5}$$

In Figure 1.5 and Figure 1.6 we find an experimental comparison between multiexponential and power-like method. We remark that in general decays from an upper energy level to the ground can be *radiative* or *non-radiative*; the difference between the two process is that radiative decays emit photons, while non-radiative don't (*intersystem crossing* is a non-radiative transition)[12].

Now we consider phosphorescence; experimentally, almost every decay trends follow similar patterns, which were carefully analyzed by the French physicist Edmond Becquerel (1820-1891). Becquerel described phosphorescence decays using an exponential of time, analogously to fluorescence decays in equation (1.1), or even a sum of two exponentials. However, in the case of inorganic solids, he obtained a better fit with the following empiric relation[3]:

$$I(t) = \frac{1}{(1 + t/c)^{\frac{1}{m}}} \ ; \tag{1.6}$$
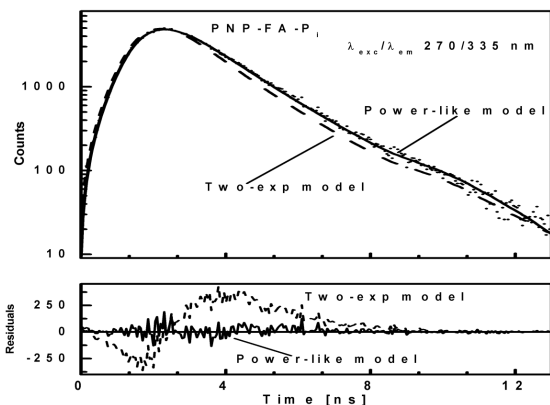
Figure 1.5: Fluorescence intensity decay ($\lambda_{exc}/\lambda_{em}$ 270/335 nm) of ternary complex of *E. coli* PNP, FA, and P$_i$ shown by dotted curve. The lower panels show residual differences between experimental and theoretical values.
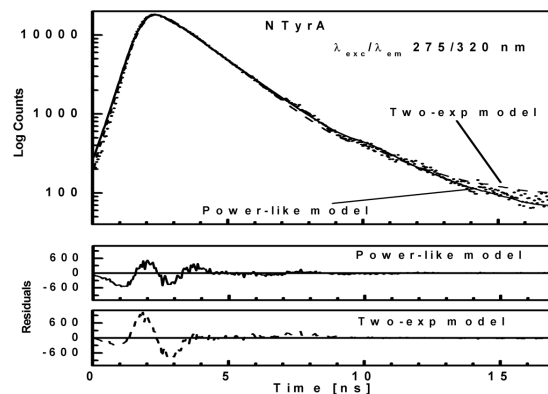
Figure 1.6: Fluorescence intensity decay ($\lambda_{exc}/\lambda_{em}$ 275/320 nm) of NATyrA shown by dotted curve. The lower panels show residual differences between experimental and theoretical values.

the equation (1.6) shows the dependence of the *normalized* intensity $I(t)$, which means that $I(0) = 1$, from time t. The terms c and m are respectively a time constant and a parameter such that $1/2 \leq m \leq 1$. When m is less than 1, this function decays faster than a hyperbola and can thus be called a *compressed* or even *squeezed* hyperbola.

1.1.2 Applications to instruments and gadgets

Fluorescence and phosphorescence are both fascinating and complex phenomena which occur spontaneously in nature. In fact, as well as the inorganic compounds even organic materials exhibit these properties. In the case of fluorescence, in order to make a material glow you normally have to use a low/medium/short wavelength UV flashlight which emits light from about 250 nm to 365 nm. That's because most of the minerals are not fluorescent enough under ($\sim$ 390 nm). It is worth mentioning a fun fact, just to present a likable aspect of fluorescence: there are plenty of "amateur explorers" who enjoy searching for fluorescent minerals and report their discoveries online. One of the main crow-founded website, whose fan base comunity even organize events and trips, is *"Nature's Rainbow: a Fluorescent Mineral SuperSite"*. In this website you can find for free an endless number of reports and precious information about these minerals. They usually use Convoy UV flashlights that allow them to recognize the relevant materials. In Table 1.1 we have a list with some *fluorescent* minerals[13] and *phosphorescent* compound[14].

Let's now look at some phosphorescence problems of the recent past; after Cascariolo,

Fluorescent materials		
Name	**Chemical formula**	**Wavelength required**
Adamite	$Zn_2(AsO_4)(OH)$	(254-365) nm
Baryte	$BaSO_4$	(254-365) nm
Calcite	$CaCO_3$	(254-365) nm
Esperite	$PbCa_3Zn_4(SiO_4)_4$	254/365 nm
Fluorite	CaF_2	(254-365) nm
Hydrozincite	$Zn_5(CO_3)_2(OH)_6$	254 nm
Wiellemite	Zn_2SiO_4	254/365 nm
Zircon	$ZrSiO_4$	254 nm
Phosphorescent materials		
Name	**Light wavelength**	**Maximum duration**
Strontium aluminate (Based) ($SrAl_2O_4$)	520 nm	$(12-20)$ h
Strontium aluminate (Based) ($Sr_3Al_2O_6$)	612 nm	$(12-20)$ h
Strontium aluminate (Based) ($SrAl_2O_7$)	480 nm	$(12-20)$ h
Calcium sulfide (CaS)	620 nm	$(1-2)$ h

Table 1.1: List of some fluorescent and phosphorescent materials. It is difficult to obtain detailed information about these phenomena, or they are overly specific for our purposes.

luminous paints were based on the luminescence emission from zinc sulfide, doped with copper (Cu). These sulfide-based materials were used in optoelectronic devices (electronic devices that interacts with light) and in catalysts. Their applications were later limited by their short *afterglow* time and low brightness. Radioactive elements such as cobalt (Co) and promethium (Pm) were codoped to enhance the luminescence duration of these sulfide-based materials. Although this doping prolonged luminescence duration, the use of radiating elements are strongly not recommended due to environmental safety issue. In addition, sulfide-based phosphors are sensitive to carbon dioxide (CO_2) and moisture and they are chemically unstable. Researches have been continued for an

Figure 1.7: Phosphorescent paint available online; it can be use to realize paintings or, sometimes, it can be apply on the body to generate some interesting effects.
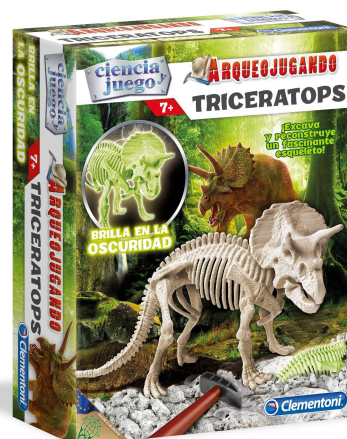
Figure 1.8: An example of a toy for children made with some phosphorescent pigments.

eco-friendly and chemically stable luminescent materials, having long after glow properties. The innovation of $SrAl_2O_4 : Eu^{2+}$, Dy^{3+} phosphor (Europium and Dysprosium) by Matsuzawa and Yamamoto in 1997[15] was the breakthrough in the field of phosphorescence. For the first time, they introduced the trivalent rare-earth ions (Dy^{3+}) as an auxiliary activators in $SrAl_2O_4 : Eu^{2+}$ (and in $CaAl_2O_4 : Eu^{2+}$) to prolong the duration of the emission. For the sake of clarity, rare-earth materials are a collection of seventeen elements of the periodic table and, despite their name, are relatively common on Earth[1]. Thus, the first group of modern luminescent complexes was the Eu^{2+}-doped and rare-earth (R^{3+}) co-doped alkaline earth aluminates. The Eu^{2+} activated strontium aluminate phosphors have long phosphorescence, higher stability (also with moisture), and quantum efficiency than the sulfide-based luminescent materials. Such materials can gain the energy or radiation from ambient solar light and can remain photoluminescent for longer period of time $(12 - 20)\,\text{h}$[14].

Luminous phenomena in art and entertainment

Phosphorescent pigments were widely commercialized all over the world and after Yamamoto's work they became quite common. Many playing cards, action figures and even paintings have been created using these luminous properties. If we think about how many priceless studies and efforts have been made to achieve this technology, it's extraordinary how casually they managed to create and distribute such highly accessible products. In Figure 1.7 and Figure 1.8 are presented two low-price items that you can actually by online. We have examples of use even in contemporary art; the American

Figure 1.9: *Brooklyn Bridge with New York - Skyline II*. Glowing painting by Tom Bacher.

Figure 1.10: *The Crown.* Glowing painting by Tom Bacher.

painter Tom Bacher (1952) has always been fascinate by phosphorescence and its uses, enough to make him wonder if it was possible to realize a glowing paint, as he declares in an interview[16]: *I got the idea to make luminous paintings 40 years ago. I was always fascinated with plastic toys that glowed in the dark and figured that whatever made plastic toys glow, maybe I could make acrylic paints glow as well. I found out what the glow chemical was and tried mixing it with paints and it worked! Since that moment, 40 years ago, every piece of art I ever made since has glowed in the dark".* In Figure 1.9 and Figure 1.10 are shown two glowing paintings made by Bacher. Unfortunately we are not able to fully appreciate the changing in light effect, but both are realized with a normal-paint background so that when the lights are turned off, the paintings give the suggestive sensation of a night town scene.

In summary, we have seen that luminescence phenomena (particularly phosphorescence), are used in entertainment both as recreation objects and as a new artistic expression.

Applications in biophysics and spectrometry

Now we shall consider a more complex field of application of luminescence, especially fluorescence. Because of the immense amount of books and papers written about scientific fluorescence application, this paragraph will be just a brief introduction about what has been mainly studied and what has been achieved. The importance of *fluorescence methods* in biology derives from few circumstances[17]: The amount of energy that they involve is sufficiently small so that they may be introduced into living systems without causing irreparable damage or undesirable side reactions, but at the same time it's sufficiently large so that individual photon detection is possible. The entire process of photoexcitation and fluorescence decay involves times that range from 10^{-12} to 10^{-7}

seconds: this time scale is of particular interest to the biologist, since it encompasses the fastest sub-molecular motions on one extreme and the rotations and translations of the large macromolecules that compose the living organisms on the other. One powerful technique is *dynamic fluorescence depolarization*; this is a method to analyze the dynamic of proteins folding on ribosomes, by anisotropy decay measurements of some fluorescence-active species[18]. Understanding how proteins achieve their native structure is of prime importance in modern biology, because protein folding is a prerequisite for cell function. The necessity of using fluorescence comes from the difficulties of studying protein folding *in vitro* and *in vivo*. Both the techniques in fact don't represent a reliable simulation of what is really going on; in vitro we can't get information about the influence that a nascent protein's native environment has on its ability to sample conformational space during and after biosynthesis, while in vivo environment may well alter the flux across different folding routes and the transient and equilibrium chain dynamics[18]. Fluorescence anisotropy decays are indeed uniquely suited to yield direct information on the local dynamics of nascent proteins. It comes by itself that understanding how proteins (and in general molecules) work will enormously help medical researches.

Fluorescence is widely used even in spectrometry to show the structure of some specific materials. In particular, the technique used for chemical analysis utilizes X-ray fluorescence (XRF), that has been drastically improved in the period from 1947 to the middle 1960s[19]. That is not to say that the more recent years have been devoid of developments, but as the field has become mature, progress becomes slower and less frequent. There are many types of X-ray fluorescent spectrometers available on the market today but most of these fall roughly into two categories, wavelength dispersive instruments and energy dispersive instruments. The first ones exploit the diffracting property of a single crystal to separate the polychromatic beam coming from the speciem, and then processing the incoming radiation to get information about the structure; this technique was introduced in the early 1950s. The second ones, a *Si(Li) detector* is utilized to give a spectrum of voltage pulses that is directly proportional to the spectrum of X-ray photon energies entering the detector. Then, an electronic voltage level sorter (multi-channel analyzer) is used to separate and collect these voltage pulses and store them in terms of their energies[19], in order to elaborate the structure of the speciem.

1.1.3 Luminescence and scattering in holograms

In the previous sections we had an introduction of photolumiescence and its area of application. Both fluorescence and phosphorescence are produced by transitions from excited energy levels to the ground one, which cause spontaneous emission. However, to date we don't have any technology that can properly manipulate these phenomena in order to generate luminous figure in space. In fact, most of the current devices utilize optical illusions or *scattering*. We now want to consider some of the few projects which don't completely use optical tricks, but that are realized by *scattering* or even with
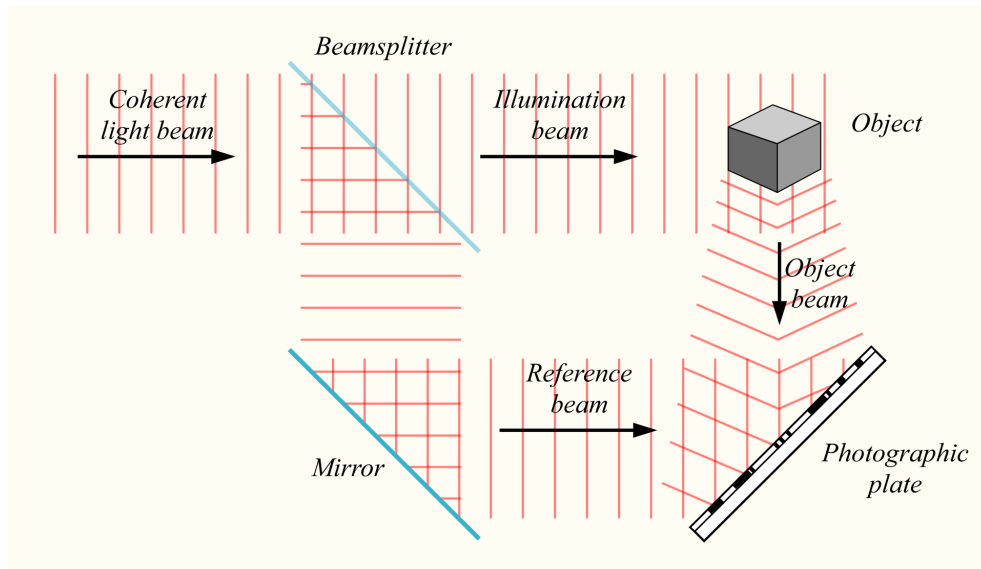
Figure 1.11: Simplified schematization of the functioning of holographic apparatus; as we can see, the light diffracted by the object and the reference beam interfere on the photographic plate.

plasma.

Holography

Let's start by saying that the popular concept of "hologram" is usually mistaken (mostly because of Star Wars) with the idea of a 3D image floating in mid air. In reality an hologram is the result of an holographic process, which consists in printing on a photographic plate the superposition of two coherent light beams: as we can see from Figure 1.11, the light beam is splitted in two by a semi-transparent glass (*beamsplitter*), then one is diffracted by the object that we want to depict, the other goes straight to the photographic plate; the result of the superposition on the plate is an image that retains some properties of the scene which are[20]:

- **Parallax**: As you change your viewpoint, the relative position of the objects appears to change as well.

- **Relative size**: Closer objects appear bigger then more distant ones.

- **Stereopsis**: The same image gets to each eye with two slightly different perspectives. The brain then processes these differences as depth. (We can test this simple property by looking at a finger close to our nose)
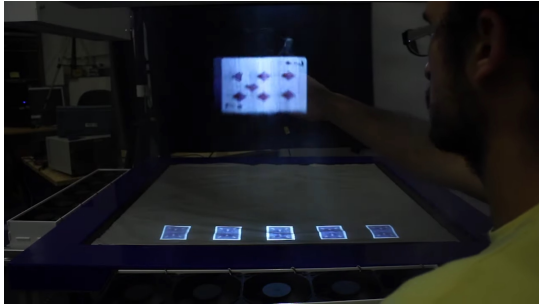
Figure 1.12: Interactive card game generated by scattering (MisTable).
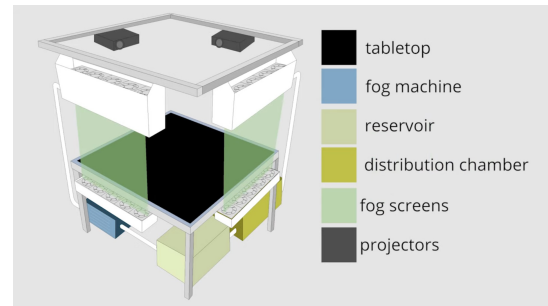
Figure 1.13: Schematization of the MisTable prototype components.

These properties are necessary to give the observer the perception of depth. As we know from physical optics, the detail of the hologram depends on the wavelength of the beam; in fact, it has to be at least comparable with the size of the object[20]. Holography was first invented by the Hungarian-British physicist Dennis Gabor (1900-1979), for which he received the Nobel Prize in Physics in 1971. He invented holography as an improvement of X-ray microscopy, using electronic waves instead of electromagnetic[21]. We have then defined what an hologram is and how can be obtained. With that in mind, we will keep using the word "hologram" to identify a 3D luminous image, for the sake of brevity.

Scattering holograms

The easiest way to explain scattering, and it will be enough for our purposes, is to imagine a process where you have a photon beam colliding with a small particle, let that be a molecule; if we don't consider photons absorption, we can say that the collision is elastic and the photons are then bouncing in any direction from the molecule. This will make the particle like a luminous point in space emitting light of the same frequency of the source. The intensity of the light reflected will be proportional to the number of particles scattered and to the intensity of the beam. With this idea attempts have been made to build a device capable of generating holograms. In general, the concept behind every device is to use a dense gas limited within a volume and properly project on it some light beam in order to generate by scattering the required image. The majority of the gas utilized are steam, or water solutions with propylene glycol, or glycerol, both non-toxic chemical compound[22]. The team of researchers BIG (*Bristol Interaction Group*) developed an interesting device which can recreate interactive images, called *MisTable*[23], like shown in Figure 1.12. We can actually see in Figure 1.13 that in this case the volume is not entirely occupied by fog, but they just used two *fog screens* with their respective projector. In order to recreate a 3D scene, they have used the possibility to go behind the image, then they properly calibrated the response of your interactions by tracking your hand movements. This is not a real hologram, but it is a clever way to utilize

scattering of light to recreate interactive scenes. The main problem with scattering is that all the particles interacting with the light beam emits at the same frequency of the incident radiation; this means that if you have a volume full of a dense gas and you just want to illuminate a single small portion of this volume, let's say in the middle, you will have to deal with the all previous and subsequent particles along the path. You could overcome this issue by utilizing plenty of weaker beams focused on the same point, so that you won't be able to perceive them singularly and the point will still be illuminate. However, is obvious that this solution is not particularly recommended. The ideal case would be to only illuminate that point, without having any interactions (or maybe not visible ones) with the rest of the volume. In the next chapter we will carefully introduce the theory required to explain a method that allows us to recreate (in theory at least) this particular situation described.

Plasma holograms
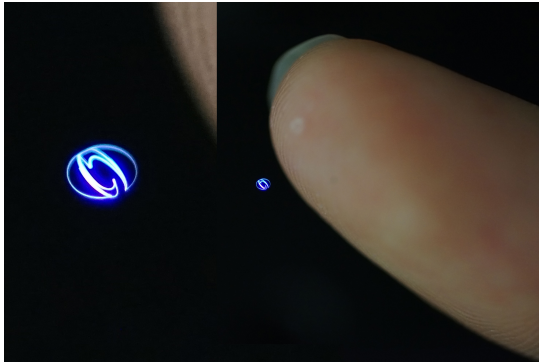
Figure 1.14: Small, but high detailed 3D hologram generated by DNG.
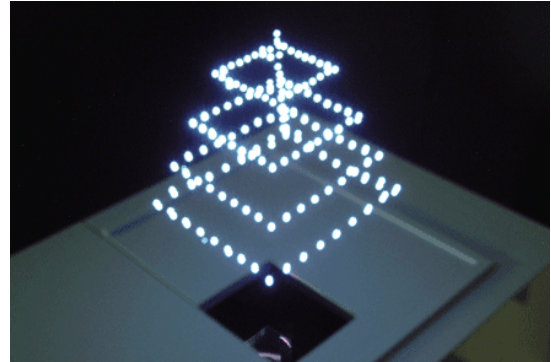
Figure 1.15: Result of a simulation of the Burton Inc. plasma hologram.

Another way to realize luminous figures in space is through a ionization process of a gas, typically by driving a an electric current through it. In fact, *plasma* is defined as a strongly ionized gas and sometimes it is considered as a fourth sate of matter; you have a solid at low temperatures, heating it up gives you a liquid, then a gas and in the end you eventually have a plasma. As we mentioned, if we want to generate plasma is not usually enough to simply heating up a container of gas. The problem is that for the most part a container cannot be as hot as a plasma needs to be in order to be ionized, or the container itself would vaporize and become plasma as well. Generally, energy is give directly to free electrons in the plasma so that electron-atom collisions liberate more electrons and the process cascades until the desired degree of ionization is achieved[24]. The two Japanese companies *Burton Inc.* and *Digital Nature Group* utilize ionized gas to create luminous 3D images, both by using high-intensity lasers focused in

small volumes. In Figure 1.14 e Figure 1.15 are showed the result of each project; as we can see, the approaches of the two companies are completely different: one wanted to generate large-sized images, the other chose to obtain high level of detail but with hardly noticeable figures. Digital Nation Group used two pulsed lasers, one at a power of 2W at 10^3 dot/s, the other 10W at $2 \cdot 10^6$ dot/s[25]. We won't dig into details, but they exhaustively explained their apparatus in the paper [25] in the references section. Unfortunately there aren't much information of Burton Inc. project, except for their website.

The result obtained with plasma holograms are worthy of interest, but this technology has real safety issues difficult to overcome because of the energy required to achieve the phenomenon.

Chapter 2

Theory behind the project

We will now discuss about the physical principles that are the main ingredients of the model for a device able to show 3D figures in space. The device has been named ODSE (*Optical Diffusion by Spontaneous Emission*). In this chapter we review briefly the atomic orbital theory retracing the main steps that lead to fine and hyperfine structure, such as hydrogen spectral lines, Stern-Gerlach experiment, Zeeman and Stark effect. Then we will tackle some processes of radiation-matter interaction, in particular the emission and absorption of photons by simple atoms. Finally, an introductory discussion on laser light generation will be given: the three level mechanism used to generate laser light will be exploited to produce at first single light spot in a gas volume and later more complex images.

2.1 Atomic orbital theory

In order to be able to make predictions about our key quantity, like the wavelength of the emitted light or the emission rate, a careful look at the quantum atomic model is required. Let's note that is not possible to find analytical solutions of the *Schrödinger problem* for multi-electrons atoms (except for helium), since their hamiltonian is not integrable; for these problems we can get just approximate solutions through a method called *perturbation theory*. We are going to describe in detail the structure of an hydrogen-like atom and then we will try to expand that model to a generic atom.

2.1.1 Bohr model

Bohr model of atom, which is an evolution of the previous one suggested by Rutherford, uses (fairly) some rough assumptions and principles formulated just to find a way around certain sperimentals problems. In fact, Bohr postulated the following properties[26]:

(a) An electron in an atom moves in a circular orbit about the nucleus under the influence of the Coulomb attraction with it and the nucleus itself.

(b) It is only possible for an electron to move in an orbit for which its orbital angular momentum L is an integer multiple of the *reduced Planck constant* $\hbar \equiv \frac{h}{2\pi}$, so where $L = n\hbar$.

(c) The total energy of the electron is conserved, despite the fact that a charge constantly accelerated.

(d) When an electron transit from an orbit of energy E_i to another orbit of energy E_f electromagnetic radiation is emitted if $E_f < E_i$; on the contrary, electromagnetic radiation is absorbed if $E_f > E_i$. The frequency of this radiation is obtained from the *Planck-Einstein* relation: $\nu = \frac{|E_i - E_f|}{h}$.

Let us consider an atom consisting of a nucleus of charge Ze, mass M and a single electron of charge $-e$ interacting through a coulombic potential

$$V(r) = -\frac{Ze^2}{4\pi\varepsilon_0 r} \ , \tag{2.1}$$

where r is the radius of the orbit. We introduce $\mu \equiv \frac{Mm_e}{M+m_e}$ as the reduced mass of the $nucleus(M) - electron(m_e)$ system, with which we write its hamiltonian

$$H = \frac{p^2}{2\mu} + V(r) = \frac{p^2}{2\mu} - \frac{Ze^2}{4\pi\varepsilon_0 r} \ . \tag{2.2}$$

Now, the coulombic potential (2.1) assures us that we are dealing with a central potential problem, therefore we can write the balance between the central force and the radial acceleration by means of the second principle of dynamics as:

$$\mu \frac{v^2}{r} = \frac{Ze^2}{4\pi\varepsilon_0 r^2} = v\frac{L}{r^2} = v\frac{n\hbar}{r^2} \ , \tag{2.3}$$

where we used (b) Bohr's postulate. From the (2.3) we can obtain the fundamental relations describing v and r in a semi-classical look:

$$v = \frac{Ze^2}{4\pi\varepsilon_0} \frac{1}{n\hbar} \ , \tag{2.4}$$

$$r = \frac{4\pi\varepsilon_0}{Ze^2\mu}(n\hbar)^2 \ . \tag{2.5}$$

In particular, if we substitute all the values listed in Appendix A with $Z = 1$ in equation(2.5), we get *Bohr radius*

$$a_0 = \frac{4\pi\varepsilon_0}{e^2\mu}(n\hbar)^2 \simeq 52.918\,\mathrm{pm} \ . \tag{2.6}$$

In Bohr model, a_0 represent the distance between the electron and the nucleus of the hydrogen atom; this result is perfectly in agreement with the latest hyperfine structure model. To calculate the energy levels, we use relation (2.2), writing the total energy by the substitution $p = \mu v$:

$$E = \frac{\mu v^2}{2} - \frac{Ze^2}{4\pi\varepsilon_0 r} = \frac{\mu}{2}\left(\frac{Ze^2}{4\pi\varepsilon_0}\frac{1}{n\hbar}\right)^2 - \mu\left(\frac{Ze^2}{4\pi\varepsilon_0}\frac{1}{n\hbar}\right)^2 = -\frac{\mu}{2}\left(\frac{Ze^2}{4\pi\varepsilon_0}\frac{1}{n\hbar}\right)^2 \ , \tag{2.7}$$

where we have used relations (2.4) and (2.5). Finally, introducing *fine-structure constant* α we get the energy levels labeled with the *principal quantum number* n in the form:

$$E_n = -\frac{\alpha\mu c^2 Z^2}{2n^2} \ , \tag{2.8}$$

with

$$\alpha \equiv \frac{e^2}{4\pi\varepsilon_0\hbar c} = \frac{e^2}{2\varepsilon_0 hc} \simeq \frac{1}{137} \ .$$

We can find all the terms and their values of the (2.8) listed in *Appendix A*. We have already pointed out that Bohr atom model is a strong simplification of the reality, but it's possible nevertheless to predict with impressive accuracy the value relative to the first energy level of the hydrogen atom ($n = 1$); in fact, substituting all the values in the equation (2.8) we obtain:

$$E_n = -\frac{13.6\,eV}{n^2} \ . \tag{2.9}$$

We verify this result by looking at the *emission spectrum* of hydrogen atom, which is shown in Figure 2.1. Without digging too much into historic details, we just mention that Thomas Melvill (1726-1753) in 1752 showed that light from incandescent gas was composed of a large number of discrete frequencies called *emission lines*[27]. It was subsequently discovered that atoms exposed to white light can only absorb light at specific frequencies, called *absorption lines*. After many studies, it was found that each atom has its own characteristic *line spectrum* and this information proved to be crucial in many fields, for example to determine the elements in the sun and stars. In the late 1800s Balmer, Rydberg and scientists began to approach the spectral line problem analytically; first in 1885 Balmer observed the hydrogen emission in the visible spectrum, then Rydberg developed an empirical formula to estimate those values, which is[30]:

$$k = Z^2 R_H \left(\frac{1}{n_1^{\ 2}} - \frac{1}{n_2^{\ 2}}\right) \ , \tag{2.10}$$
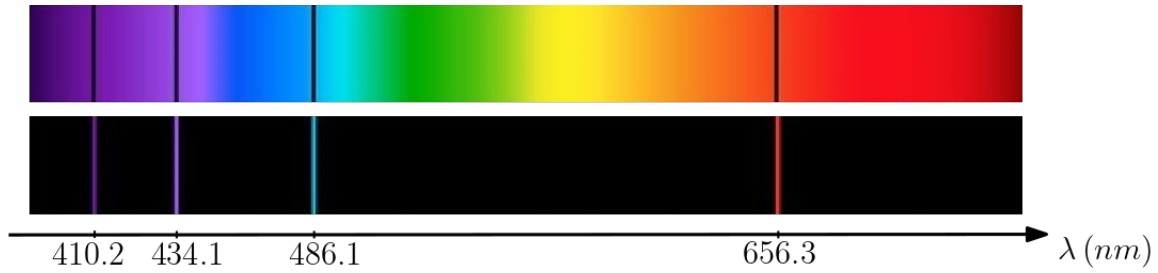
Figure 2.1: Representation of absorption (top) and emission (bottom) spectral lines of hydrogen atom. The values of the wavelength are the first four terms of Blamer series, which are approximately in visible spectrum.

Name	Wavelength ranges	Formulas	Index
Lyman (1906)	Ultraviolet	$k = R_H \left(1 - \frac{1}{n^2}\right)$	$n = 2, 3, 4, ...$
Balmer (1885)	Near ultraviolet/visible	$k = R_H \left(\frac{1}{2^2} - \frac{1}{n^2}\right)$	$n = 3, 4, 5, ...$
Paschen (1908)	Infrared	$k = R_H \left(\frac{1}{3^2} - \frac{1}{n^2}\right)$	$n = 4, 5, 6, ...$
Brackett (1922)	Infrared	$k = R_H \left(\frac{1}{4^2} - \frac{1}{n^2}\right)$	$n = 5, 6, 7, ...$

Table 2.1: Empirical series for hydrogen spectral lines. The value k is the wavenumber $1/\lambda$. The term R_H is an empirical constant called *Rydberg constant* for hydrogen; its value is listed in Appendix A. It is also reported the year when the series was first observed [26] [27].

where k is the wavenumber defined as $1/\lambda$, Z is the atomic number, R_H is Rydberg constant (Appendix A), n_1 and n_2 are the principal quantum number of the two energy levels involved in the transition, with $n_1 \leq n_2$ for obvious reasons. In Figure 2.2 are illustrated the first six terms obtained with the equation (2.9) and in Figure 2.3 are shown fours series of hydrogen spectral lines. If we want to estimate the accuracy of Bohr model for the first terms, we can confront the predicted wavelength value of the first emission with the one given empirically by Leyman series. We obtain the energy difference between the energy levels relative to $n = 1$ and $n = 2$ from equation (2.9):

$$E_{2 \to 1} = \left(13.6 - \frac{13.6}{2^2}\right) \text{eV} = 10.2 \, \text{eV} . \tag{2.11}$$
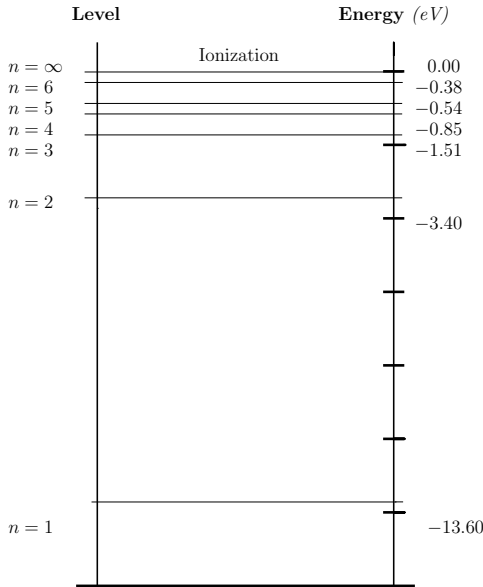
Figure 2.2: Graphic representation of hydrogen energy levels by using the relation obtained with Bohr model of atoms.
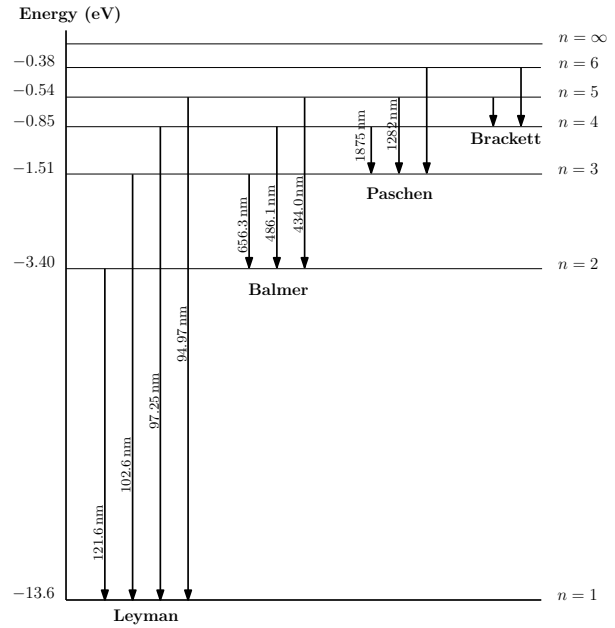
Figure 2.3: The spectrum of atomic hydrogen. The only series relative to the visible wavelength emissions is *Balmer series*, the other ones are over and below visible spectrum. The scales are exaggerated for the sake of clarity.

Now we evaluate the wavelength of the photons involved in this transition by Planck-Einstein relations:

$$\lambda = \frac{c\,h}{E_{2\to1}} = 121.6\,\text{nm} \ , \tag{2.12}$$

where we have substituted all the values listed in Appendix A. we can derive the experimental value observed from Lyman series in Table 2.1 by taking the inverse, which is in fact 121.6 nm and correspond perfectly; however, if we repeat the process considering the visible transition between $n = 2$ and $n = 3$ (first Balmer series term) we obtain:

$$\lambda = \frac{c\,h}{E_{3\to2}} = 667.0\,\text{nm} \ , \tag{2.13}$$

from which we can already see a 2% difference between the value obtained and the one experimentally observed. We conclude that Bohr model of atom achieved important results for a better understanding of the structure of atoms, but it is clearly immature to properly explain radiative phenomena. Also, the energy levels predicted by the (2.9) are not all the possible ones, as we will see in the next section.

2.1.2 Towards quantum mechanics

Before we introduce the theory of fine structure of atoms we shall take a quick look at the historical background; it's not of primary importance to solve completely the following problems, what matters is to give as best we can the chronological order of the various discoveries and experiments. We said in the previous paragraph that the energy levels given by Bohr's formula (2.9) are not all the possible ones; this was very well observed by the Dutch physicist Pieter Zeeman (1865-1943) who was the first in 1896 to examine what is today known as *Zeeman effect*; this phenomenon was crucial for the understanding of *energy level degeneracy* and the development of quantum mechanics. The *Zeeman effect* consists in splitting a spectral line into discrete components as the result of an interaction with a weak static magnetic field [27]. This discovery suggested that energy levels should have had more layers than the ones known at that time. Today we would say that a generic system is identified by specific quantum states, each labeled with a set of quantum numbers such as n, and if an energy level corresponds to two or more quantum states then it is degenerate. Zeeman in his experiment observed that the spectral lines were splitted in evenly spaced sub-lines as shown in Figure 2.4 and Lorentz even

managed to explain part of the phenomenon in terms of a classical theory [26]. One year later, the scientist Thomas Preston (1860-1900) found out that in general cases those splits were more chaotic and Lorentz theory couldn't predict them. Those unexplained cases were called *Anomalous Zeeman effects*; in reality, both are exactly the same physical phenomenon, whose different behavior is due to the intensity of the magnetic field used.. With the introduction of *orbital angular momentum* **L** and *spin* **S** it is easily explainable. For now we just say that in an atom (or molecule) there are reasonably strong internal magnetic fields ($\sim 1\,\mathrm{T}$) that interact with the moving electrons and therefore defining a specific internal structure, in particular a *magnetic dipole moment* μ_B and a *spin magnetic moment* μ_S; in addition, spin

Figure 2.4: Representation of photographic plates showing the splitting of spectral lines in the normal and anomalous Zeeman effect (up) and Paschen-Back effect (below). The normal was the only possible split predicted by Lorentz.

and orbital angular momentum interact with each other generating a term called *spin-orbit interaction*, that constitute a specific bound between **L** and **S**. When an external magnetic field perturbs the atom (or molecule) the two dipole moments interact with it,

removing the degeneracy of the energy levels involved and forcing them to split. The difference between normal and anomalous Zeeman effect is just due to the different quantum numbers defining the states in the same energy level, in particular we can say that every *singlet* level is splitted in three lines and only depends on the orbital quantum number, the others depends on the combination of orbital and spin contributions. Now, Zeeman used weak magnetic field and the splits were extremely small; in 1921 the two physicists Friedrich Paschen (1865-1947) and Ernst Back (1881-1959) repeated the experiment using a magnetic field stronger than the one inside the atom (greater than $1\,\mathrm{T}$) and reported that with such fields the only noticeable phenomenon was the standard *Zeeman effect*; that happens because the external magnetic field interferes with the spin-orbit interaction and by doing so it reintroduce the degeneracy due to that interaction. In 1913 analogous experiment leaded by the German physicist Johannes Stark (1874-1957) was made replacing the magnetic field with an static electric field and he observed a splitting and also shifting of spectral lines of atoms; this took the name of *Stark effect*. These phenomena remained unexplained until the introduction of *spin* and *spin-orbit interaction* after 1924 thanks to Wolfgang Pauli (1900-1958) as he explained in his Nobel lecture in 1946[31].

The first attempt to correct Bohr model and explain spectral lines splitting was made by the German theoretical physicist Arnold Sommerfeld (1868-1951), who developed an empirical method that allowed him to discretize coordinates that were periodic functions of time (*Wilson-Sommerfeld quantization rule*). He managed to introduce a second and a third quantum numbers, l and m_l, known as *orbital* and *magnetic* quantum numbers respectively. The new model, which took the name *Bohr-Sommerfeld model* (also known as *old quantum theory*), gave a first explanation of normal Zeeman and Stark effects and introduced the idea of the *fine structure* of spectral lines. Sommerfeld showed that the total energy of an electron in an orbit is equal to[26]:

$$E_{n,l} = E_n \left[1 + \frac{Z^2 \alpha^2}{n^2} \left(\frac{n}{l+1} - \frac{3}{4} \right) \right] , \tag{2.14}$$

where the quantum number l satisfy the relation $l = 0, \ldots, (n-1)$. The Bohr-Sommerfeld model was a great achievement for the development of quantum theory. However, observation of the spectral lines showed that some transition predicted by the model were not found on the spectrum, like the one shown in Figure 2.5. To counterbalance this unexplained issue, it has been empirically derived a simple method to recognize the possible transitions from the forbidden ones, which took the name of *selection rule*. The rule states that the transition only occur if the following relation holds:

$$l_i - l_f = \pm 1 , \tag{2.15}$$

where the subscripts i and f represent respectively the initial and the final orbital quantum number[27]. We shall repeat the comparison between the hydrogen experimental
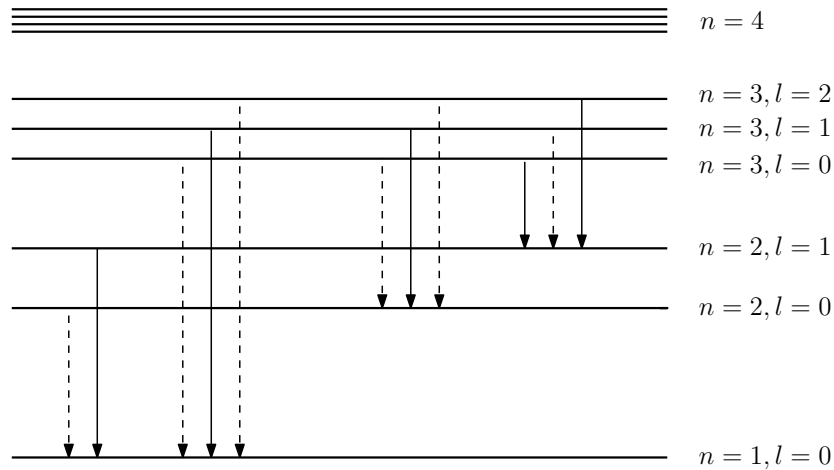
Figure 2.5: The fine-structure of some energy levels of the hydrogen atom. The splitting is greatly exaggerated for the sake of understanding. The dashed lines are the transitions that do not occur experimentally.

values of wavelength emission with the ones obtained with the equation (2.14), as we did with Bohr model. Let's consider the first transition shown by Balmer series between the energy levels relative to $n = 3$ and $n = 2$ that emits light with a wavelength of $656.3\,\text{nm}$. Proceeding in the same way as we did in the previous paragraph, we write the energy gap between the levels, considering both with $l = 0$ and $Z = 1$:

$$E_{3 \to 2} = \left(\frac{13.6}{3^2} \left[1 + \frac{\alpha^2}{3^2} \left(\frac{3}{1} - \frac{3}{4} \right) \right] - \frac{13.6}{2^2} \left[1 + \frac{\alpha^2}{2^2} \left(\frac{2}{1} - \frac{3}{4} \right) \right] \right) \text{eV} = 1.8889\,\text{eV} ,$$
(2.16)

with the associated wavelength given by *Planck-Einstein* relations:

$$\lambda = \frac{c\,h}{E_{3 \to 2}} = 656.9\,\text{nm} .$$
(2.17)

If we confront the value obtained with the one given by Balmer series, which is $656.3\,\text{nm}$, we can already see the remarkable accuracy gained with Sommerfeld quantization.

2.1.3 Fine structure of atoms

Now it's time to properly introduce the modern theory that rigorously explains the structure of atoms and the transitions between energy levels.

Schrödinger equation

We know from quantum mechanics that *Schrödinger wave function* Ψ represents a statistical *ensemble* of copies of quantum particles, which encodes all the information we

need to investigate particles behavior[29]; this function is given by the following linear differential equation, known as *Schrödinger equation*:

$$i\hbar \frac{\partial \Psi(\mathbf{r},t)}{\partial t} = \left[-\frac{\hbar}{2m}\nabla^2 + V(\mathbf{r},t) \right] \Psi(\mathbf{r},t) \;, \tag{2.18}$$

or written in the general form using Dirac algebra notation:

$$i\hbar \frac{\partial}{\partial t} \left| \Psi(t) \right\rangle = \hat{H} \left| \Psi(t) \right\rangle \;, \tag{2.19}$$

where $\hat{H}$ is the hamiltonian operator. For obvious reasons we won't be able to explore the theory behind Schrödinger and Dirac's works, but we will only recall some of their important conclusions. In easier terms, $\Psi(\mathbf{r},t)$ is a wave function relative to a single particle under the influence of a time-dependent potential $V(\mathbf{r},t)$ defined in the configuration space $\mathbb{E}^3$; according to Born's statistical interpretation the $\Psi(\mathbf{r},t)$ square module gives the probability of finding the particle in a generic region σ in configuration space at time t [28]:

$$\int_\sigma d^3x \, \Psi^*(\mathbf{r},t)\Psi(\mathbf{r},t) = \int_\sigma d^3x \, |\Psi(\mathbf{r},t)|^2 \leq 1 \;, \tag{2.20}$$

with the necessary normalized condition when we expand σ to the whole space:

$$\int_{\mathbb{E}^3} d^3x \, \Psi^*(\mathbf{r},t)\Psi(\mathbf{r},t) = \int_{\mathbb{E}^3} d^3x \, |\Psi(\mathbf{r},t)|^2 = 1 \;. \tag{2.21}$$

Now, if we consider an time-independent potential $V(\mathbf{r})$ we notice that Schrödinger equation becomes a differential equation with separable variables, so we look for a factorized solution in the form:

$$\Psi(\mathbf{r},t) = \phi(\mathbf{r})\psi(t) \;. \tag{2.22}$$

In particular equation (2.18) must hold for every value of $\mathbf{r}$ and t, therefore with the factorization we conclude that the following equations must be constant:

$$i\hbar \frac{1}{\psi(t)} \frac{d\psi(t)}{dt} = E \;, \tag{2.23}$$

$$-\frac{\hbar^2}{2m}\nabla^2 \phi(\mathbf{r}) + V(\mathbf{r}) = E \;, \tag{2.24}$$

where we have substituted the solution (2.22) in (2.18) and named the constant value E, which has the dimension of an energy. It's easy to obtain the solution of equation (2.23) by a simple integration that gives the phase

$$\psi(t) = e^{-iEt/\hbar} \;. \tag{2.25}$$

Finally, we rewrite the fundamental equation (2.24) in the usual form

$$\left[-\frac{\hbar^2}{2m}\nabla^2 + V(\mathbf{r})\right]\phi(\mathbf{r}) = E\phi(\mathbf{r}) \ , \tag{2.26}$$

that can be written even in Dirac algebra notation:

$$\hat{H}\left|\Psi\right\rangle = \left|\Psi\right\rangle E \ . \tag{2.27}$$

Equation (2.26) is called the *time-independent Schrödinger equation* and it's of primary interest in determining atomic orbital structure; it is even the irreducible form of the problem, if we want to go further we need to specify $V(\mathbf{r})$ [28]. The solution $\phi(\mathbf{r})$ to the time-independent Schrödinger problem is called *energy eigenfunction* of the *energy eigenvalue* E and it determines the stationary state of the system analyzed. We can have more eigenfunctions $\phi_1(\mathbf{r}), .., \phi_N(\mathbf{r})$ belonging to the same eigenvalue E and when it happens we said that $\phi_1(\mathbf{r}), .., \phi_N(\mathbf{r})$ are *degenerate*. It is important to notice that an eigenfunction can't be the zero function, as it determinate the probability of finding a particle and so it can't vanish.

Now, in general the wave function $\Psi(\mathbf{r}, t)$ can be expanded in the following way by superposition principle:

$$\Psi(\mathbf{r}, t) = \sum_{n_d} \int dn_c \, c_n \Psi_n(\mathbf{r}, t) \ ; \tag{2.28}$$

where n_d are discrete indexes and n_c are continuous; the separable solutions themselves

$$\Psi_n(\mathbf{r}, t) = \phi_n(\mathbf{r})e^{-iE_n t/\hbar} \tag{2.29}$$

therefore encode all probabilities and expectation values that do not depends on time because of the exponential factor, a property that is not shared by the general solution of (2.18). From this time independence property comes the name *stationary state*.

Hydrogen-like atoms

Now we have the possibility to obtain the wave function of a generic quantum particle by solving Schrödinger equation (2.18) and with that its spatial distribution. The difficulty of the problem is due to the expression of the interaction potential $V(\mathbf{r}, t)$, which is non trivial for most of the problems we can consider. Fortunately we can set the Schröedinger problem for an hydrogen-like atom and completely solve it. In fact, we consider a time-independent coulombic potential

$$V(r) = \frac{-Ze^2}{4\pi\varepsilon_0\sqrt{x^2 + y^2 + z^2}} = \frac{-Ze^2}{4\pi\varepsilon_0 r} \ , \tag{2.30}$$

where for convenience we use spherical coordinates

$$\begin{cases} x = r\sin\theta\cos\varphi \\ y = r\sin\theta\sin\varphi \\ z = r\cos\theta \end{cases}$$

that transform the Laplacian operator ∇^2 in the following expression:

$$\nabla^2 = \frac{1}{r^2}\frac{\partial}{\partial r}\left(r^2\frac{\partial}{\partial r}\right) + \frac{1}{r^2\sin\theta}\frac{\partial}{\partial\theta}\left(\sin\theta\frac{\partial}{\partial\theta}\right) + \frac{1}{r^2\sin^2\theta}\frac{\partial^2}{\partial\varphi^2} \ . \tag{2.31}$$

If we rewrite the time-independent Schrödinger equation (2.26) in spherical coordinates we can easily notice the absence of mixed derivative terms; this suggests a natural ansatz for its solution

$$\phi(r,\theta,\varphi) = R(r)\Theta(\theta)\Phi(\varphi) = R(r)Y(\theta,\varphi) \ , \tag{2.32}$$

which can be trivially verified. Since we are dealing a central potential, we can use the *effective potential* to simplify our discussion:

$$V_{eff}(r) = V(r) + \frac{\mathbf{L}^2}{2\mu r^2} \ , \tag{2.33}$$

which contains the repulsive centrifugal force in addition to $V(r)$. Leaving the details to a quantum mechanics book, the solution (2.32) that describes the stationary states of an hydrogen-like atom is expressed as the product of a radial term $R_{n',l}(r)$ and an angular one $Y_{l,m_l}(\theta,\varphi)$. The Schrödinger equation (2.26) for a hydrogen-like atom becomes:

$$\left[-\frac{\hbar^2}{2\mu}\nabla^2 - \frac{Ze^2}{4\pi\varepsilon_0 r}\right]R_{n',l}(r)Y_{l,m_l}(\theta,\varphi) = ER_{n',l}(r)Y_{l,m_l}(\theta,\varphi) \ , \tag{2.34}$$

with ∇^2 given by (2.31). Now, the angular term must satisfies the following eigenvalue equations:

$$\begin{cases} \mathbf{L}^2 Y_{l,m_l}(\theta,\varphi) = l(l+1)\hbar^2\, Y_{l,m_l}(\theta,\varphi) \\ L_z Y_{l,m_l}(\theta,\varphi) = m_l\hbar^2\, Y_{l,m_l}(\theta,\varphi) \end{cases} \tag{2.35}$$

that show the possible values of the magnitude of angular momentum $\mathbf{L}$ and explain us the meaning of the subscripts; in fact $Y_{l,m_l}(\theta,\varphi)$ depends on the orbital quantum number l and on the new one m_l, which indicates the third component of the angular momentum $\mathbf{L}$. $Y_{l,m_l}(\theta,\varphi)$ are known functions called *spherical harmonics*. Finally, substituting (2.30) and (2.31) in (2.26) and using the quantization relation of $\mathbf{L}^2$ given by (2.35), we obtain the radial Schrödinger equation that defines $R_{n',l}(r)$:

$$\left\{-\frac{\hbar^2}{2\mu}\left[\frac{1}{r^2}\frac{d}{dr}\left(r^2\frac{d}{dr}\right) - \frac{l(l+1)}{r^2}\right] - \frac{Ze^2}{4\pi\varepsilon_0 r}\right\}R_{n',l}(r) = ER_{n',l}(r) \ . \tag{2.36}$$

The energy levels relative achievable from this models are given as follows:

$$E_{n',l} = -\frac{\mu}{2}\left(\frac{Ze^2}{4\pi\varepsilon_0\hbar}\right)^2\left(\frac{1}{l+n'+1}\right)^2 \equiv -\frac{\mu}{2}\left(\frac{Ze^2}{4\pi\varepsilon_0\hbar}\right)^2\left(\frac{1}{n}\right)^2 , \qquad (2.37)$$

where we have defined the already known *principal quantum number* as $n = n'+l+1$[29]; we list now the values of the indexes:

$$\begin{cases} n' = 0, 1, ..., +\infty , \\ l = 0, 1, ..., n-1 , \\ m_l = -l, -l+1, ..., l . \end{cases}$$

From Schrödinger model we conclude that the predicted energy levels are exactly the same as Bohr model, but with a crucial difference: each energy level is n^2 times degenerate, therefore to every level correspond n^2 different quantum states. Unfortunately, this degeneracy does not occur, because there are small differences in energy between the levels corresponding to the same principal quantum number.

Magnetic interaction

In addition to Schrödinger analysis, we have to consider that a charge who is moving around a nucleus produces a magnetic field. We will approach the problem in a classical way,
but it is possible to obtain the same results with quantum mechanics. It is true that the angular momentum **L** in a central field problem is express as:

$$\mathbf{L} = m_e(\mathbf{r} \times \mathbf{v}) = m_e vr\,\hat{\mathbf{n}} , \qquad (2.38)$$

where $\hat{\mathbf{n}}$ is the unitary vector perpendicular to the oriented surface **A** defined by the circular orbit. It's useful to assume the presence of a magnetic dipole with its relative magnetic dipole moment $\boldsymbol{\mu_l} = i\mathbf{A}$, which results antiparallel to **L** because of the negative charge of the electron, as shown in Figure 2.6. Now, if we indicate the current i as the result of the charge $-e$ which runs along a circumference of $2\pi r$ with a constant speed v, by using (2.38) we obtain:

$$\frac{\mu_l}{L} = \frac{iA}{L} = \frac{(ev)\,\pi r^2}{(2\pi r)\,m_e vr} = \frac{e}{2m_e} \equiv \frac{g_l\,\mu_b}{\hbar} . \qquad (2.39)$$
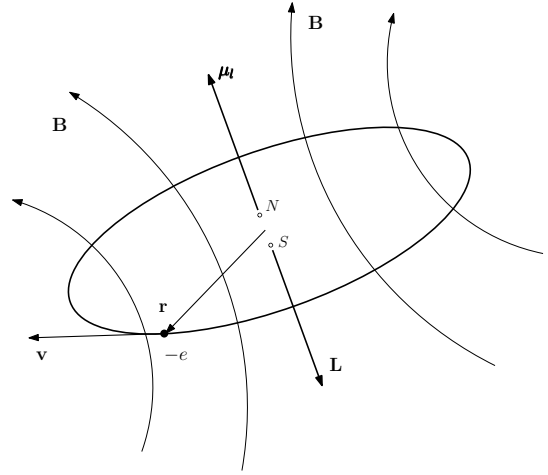
Figure 2.6: Representation of the orbital angular momentum **L** and the magnetic dipole moment $\boldsymbol{\mu_l}$ of an electron $-e$ moving in a circular orbit. The fictitious magnetic dipole is indicated by its poles N and S.

We see that the ratio between magnetic dipole moment and angular momentum is a universal constant; it is common to express the ratio using *Bohr magneton* μ_b (Appendix A) and the *orbital g-factor* g_l, where in this case is equal to 1. From relation (2.39) and in agreement with the considerations on the directions of $\boldsymbol{\mu_l}$ and $\mathbf{L}$ we have:

$$\boldsymbol{\mu_l} = -\frac{g_l \mu_b}{\hbar} \mathbf{L} \ . \tag{2.40}$$

Using the quantization relation of the angular momentum obtained in (2.35), we get:

$$\begin{cases} \mu_l = \frac{g_l \mu_b}{\hbar} \sqrt{l(l+1)}\hbar = g_l \mu_b \sqrt{l(l+1)} \\ \mu_{l_z} = -\frac{g_l \mu_b}{\hbar} m_l \hbar = -g_l \mu_b m_l \end{cases} \tag{2.41}$$

expressing the magnitude and the third component of the dipole moment $\boldsymbol{\mu_l}$ in quantum mechanics. Finally, we know from electromagnetism that a magnetic dipole placed in an magnetic field has a potential energy

$$U_L = -\boldsymbol{\mu_l} \cdot \mathbf{B} \tag{2.42}$$

and it's easy to demonstrate that if $\mathbf{B}$ varies in one direction in space (let's say z), the force acting on the dipole is:

$$F_z = -\nabla U = \frac{\partial B_z}{\partial z} \mu_{l_z} = \frac{\partial B_z}{\partial z} \left(-g_l \mu_b m_l \right) \ . \tag{2.43}$$

Stern-Gerlach experiment and the discovery of spin

The last experiment before a formal introduction of spin in quantum mechanics was made by the German physicists Otto Stern (1888-1969) and Walther Gerlach (1889-1979) in 1922. In fact, they realized a simple apparatus, like the one reported in Figure 2.7, which was able to verify the spatial quantization of $\mathbf{L}$ and $\boldsymbol{\mu_l}$. However, the measures were different from the expected values; if we look at the force given by (2.43) it's clear that the splitting lines should always be an odd number, in particular with one in the middle, since $m_l = -l, -l+1, .., 0, .., l$. The explanation to this phenomenon was that in the atom there must be another angular momentum that followed quantization rules like the ones seen for $\mathbf{L}$. That momentum took the name of *spin* $\mathbf{S}$, indicated as follow:

$$\begin{cases} S = \sqrt{s(s+1)}\hbar \\ S_z = m_s \hbar \end{cases} \tag{2.44}$$

with its magnetic dipole moment $\boldsymbol{\mu_s}$

$$\begin{cases} \boldsymbol{\mu_s} = -\frac{g_s \mu_b}{\hbar} \mathbf{S} \\ \mu_{s_z} = -g_s \mu_b m_s \end{cases} \tag{2.45}$$

where in this case s is the *spin quantum number*, m_s is the quantum number relative to the value of the third component of $\mathbf{S}$, which experimentally is equal to $\pm 1/2$ for electrons, and g_s is the *spin g-factor*, whose value depends on the quantum state considered.
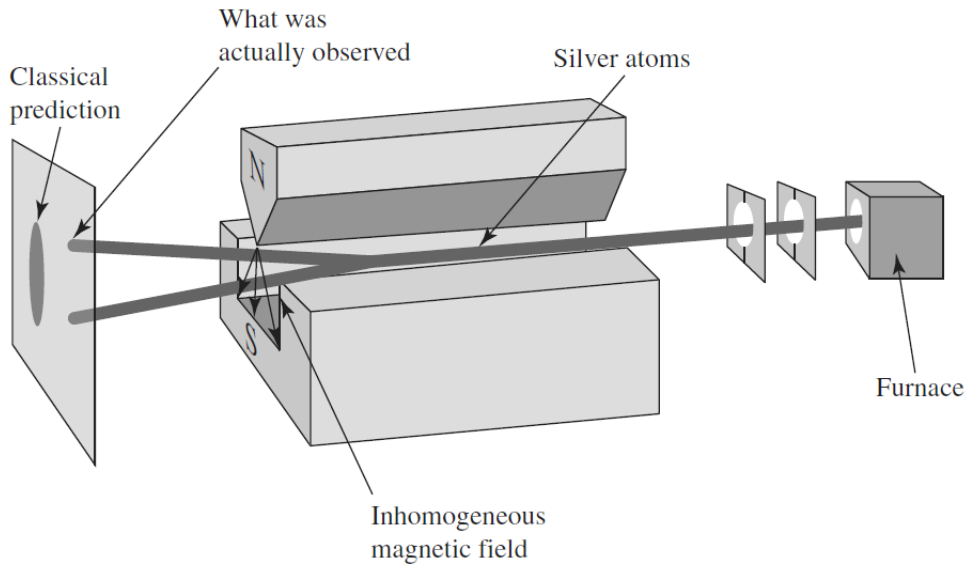
Figure 2.7: Schematization of Stern-Gerlach experimental apparatus. The result highlights that there must be another magnetic dipole moment in addition to the angular one, since a splitting occurred even if it was unexpected.

Spin-orbit interaction

Spin introduction by Pauli's suggestion was of tremendous help for the study of atomic and molecule structure; for instance, spin allowed to perfectly determine the permitted transitions between the levels and it doubles the number of electrons to populate the quantum states of multi-electrons atoms, property that goes under the name *Pauli exclusion principle*. Now, in order to calculate the interaction between the angular and the spin momentum we consider the potential energy (2.42) of a magnetic dipole immersed in a magnetic field generated by the moving electron, but using the spin magnetic dipole moment $\boldsymbol{\mu_s}$:

$$U_S = -\boldsymbol{\mu_s} \cdot \mathbf{B} . \tag{2.46}$$

Using relation (2.45) we obtain

$$U_S = \frac{1}{2} \frac{g_s \mu_b}{\hbar} \mathbf{S} \cdot \mathbf{B} , \tag{2.47}$$

with the factor $1/2$ given by a relativistic effect called *Thomas precession*. We want to express the potential energy in terms of **S** and **L**, so we use the following expressions:

$$\mathbf{B} = -\frac{1}{c}\mathbf{v} \times \mathbf{E} , \tag{2.48}$$

$$\mathbf{F} = -e\mathbf{E} , \tag{2.49}$$

$$\mathbf{F} = -\frac{dV(r)}{dr}\frac{\mathbf{r}}{r} ; \tag{2.50}$$

With these relations we get an easy expression of the magnetic field produced by the moving electron:

$$\mathbf{B} = -\frac{1}{ec^2r}\frac{dV(r)}{dr}\mathbf{v} \times \mathbf{r} = \frac{1}{emc^2r}\frac{dV(r)}{dr}\mathbf{L} , \tag{2.51}$$

where we used the known relation $\mathbf{L} = \mathbf{r} \times m\mathbf{v} = -m\mathbf{v} \times \mathbf{r}$. Finally, by substituting (2.1.3) in relation (2.47) we obtain the energy interaction between **L** and **S** as follow:

$$U_{SO}(r) = \frac{g_s\mu_b}{2\hbar emc^2 r}\frac{dV(r)}{dr}\mathbf{S} \cdot \mathbf{L} = \frac{1}{2m^2c^2 r}\frac{dV(r)}{dr}\mathbf{S} \cdot \mathbf{L} , \tag{2.52}$$

that can be rewritten using quantization relations and angular momentum theory as:

$$\langle U_{SO} \rangle = \xi \left(\frac{j(j+1) - l(l+1) - s(s+1)}{2} \right) , \tag{2.53}$$

where ξ can be measured experimentally. Spin-orbit interaction is responsible for the removal of **J** degeneracy and so for the fine-structure of atom, where $\mathbf{J} = \mathbf{L} + \mathbf{S}$ is the total angular momentum. Equation (2.52) is the general form of spin-orbit interaction, because the potential $V(r)$ is not evaluated; if we have the internal potential interaction, it can even be applied to multi-electron atoms. For an hydrogen-like atom, we use the potential energy given by equation (2.30) and we simply get:

$$U_{SO} = \frac{e^2}{2(4\pi\epsilon_0)em^2c^2r^3}\mathbf{S} \cdot \mathbf{L} . \tag{2.54}$$

Without given any demonstration, we report the general equation of the complete one-electron atom hamiltonian, called *Dirac equation*:

$$H = H_0 + H_1 + H_2 + H_3 =$$
$$= \left[\frac{p^2}{2\mu} + V(r) \right] + \left[-\frac{p^4}{8\mu^3c^2} \right] + \left[\frac{1}{2\mu^2c^2}\frac{dV(r)}{r}\frac{dV(r)}{dr}\mathbf{S} \cdot \mathbf{L} \right] + \left[\frac{\pi\hbar^2}{2\mu^2c^2}\frac{Ze^2}{4\pi\epsilon_0}\delta(\mathbf{r}) \right] , \tag{2.55}$$

where appear two new terms, H_1 and H_3, which are purely relativistic corrections; those corrections are called respectively *Thomas relativistic correction* and *Darwin term*; this

very last one is orthogonal to the spin-orbit interaction since it only appears when $\mathbf{L} = 0$. If we evaluate the contribution of all the terms in equation (2.55) by using *perturbative theory*, we obtain the total energy eigenvalue:

$$E_{n,j} = E_n \left[1 + \frac{Z^2 \alpha^2}{n^2} \left(\frac{n}{j + 1/2} - \frac{3}{4} \right) \right] , \qquad (2.56)$$

where j is the quantum number relative to the total angular momentum $\mathbf{J} = \mathbf{L} + \mathbf{S}$, such that:

$$\begin{cases} j = |L - S|, ..., L + S , \\ m_j = -j, -j + 1, ..., j . \end{cases}$$

Now, as we can see in relation (2.56) the energy levels depend on the quantum number j; this implies that each level with $l \neq 0$ will be splitted in j components of different energy, thanks to the spin-orbit interaction. As we have already seen in relation (2.15), it has been empirically shown that some transitions occur, while other don't. We could even justify it now, but we will simply list the full *selection rules* now that we have more energy levels, which are:

$$\begin{cases} \Delta L = \pm 1 \ (\Delta L = 0 \ \text{only if it's not an electron transition}) \\ \Delta J = 0, \pm 1 \ (\text{transitions from levels with } J_i = J_f = 0 \text{ are not allowed}) \\ \Delta m_j = 0, \pm 1 . \end{cases} \qquad (2.57)$$

2.2   Multi-electrons atom

Let's consider a generic multi-electron atom with N electrons and an atomic number of Z; we write its hamiltonian in atomic units:

$$H = -\sum_{i=1}^{N} \left(\frac{\nabla_i^2}{2} \right) - \sum_{i=1}^{N} \left(\frac{Z}{r_i} \right) + \sum_{i=1}^{N} \sum_{j=1, i<j}^{N} \left(\frac{1}{r_{ij}} \right) , \qquad (2.58)$$

which are in order kinetic, coulombic attractive and repulsive terms. In order to solve the Schrödinger problem, we have to use what is known as *central field approximation*, since the repulsive terms are too intense to be considered a perturbation. If we subtract the central interactions from the repulsive terms we can however define a new central potential as the result of the sum of the attractive and repulsive central terms, leaving some small interactions that can now be treated with *variational method*. We begin writing the hamiltonian for the i-th electron as:

$$H = H_c + H_1 = -\left(\frac{\nabla_i^2}{2} \right) - \left(\frac{Z}{r_i} \right) + \sum_{j=1, j \neq i}^{N} S(r_i) + \sum_{j=1, i<j}^{N} \frac{1}{r_{ij}} - \sum_{j=1, j \neq i}^{N} S(r_i) , \quad (2.59)$$

and then we isolate the central terms:

$$H_c = -\left(\frac{\nabla_i^2}{2}\right) - \left(\frac{Z}{r_i}\right) + \sum_{j=1,j\neq i}^{N} S(r_i) , \qquad (2.60)$$

where $S(r_i)$ are the mean value of the central interactions on the i-th electron from the repulsive terms. In order to evaluate $S(r_i)$ we use *Hartree iterative method*: we evaluate the central eigenfunction $u_{\alpha,i}(\mathbf{r}_j)$ to get $S(r_i)$, and then we solve the central hamiltonian problem obtaining a new central eigenfunction that allows us to calculate again $S(r_i)$ as follow:

$$S(r_i) = \sum_{j=1,j\neq i}^{N} \int u_{\alpha,i}^* \frac{1}{r_{ij}} u_{\alpha,i} = \sum_{j=1,j\neq i}^{N} \langle u_{\alpha,i}(\mathbf{r}_j)|\frac{1}{r_{ij}}|u_{\alpha,i}\rangle (\mathbf{r}_j) , \qquad (2.61)$$

which we evaluate experimentally the first time to begin the iteration, then we solve the central hamiltonian problem:

$$\left[-\left(\frac{\nabla_i^2}{2}\right) - \left(\frac{Z}{r_i}\right) + \sum_{j=1,j\neq i}^{N} \langle u_{\alpha,i}|\frac{1}{r_{ij}}|u_{\alpha,i}\rangle\right] u_{\alpha,i}(\mathbf{r}_j) = E_{\alpha,j} u_{\alpha,i}(\mathbf{r}_j) , \qquad (2.62)$$

which finally gives us $u_{\alpha,i}(\mathbf{r}_j)$. We continue this process until we're satisfied with the precision obtained. Now we can proceed writing the total central eigenfunction of the problem with a useful tool known as *Slater determinant*; we first write it down and then we discuss it:

$$\psi_c(\mathbf{q}) = \frac{1}{\sqrt{N!}} det \begin{bmatrix} u_{\alpha_0}(\mathbf{q}_1) & \dots & u_{\alpha_N}(\mathbf{q}_1) \\ \vdots & \ddots & \vdots \\ u_{\alpha_0}(\mathbf{q}_N) & \dots & u_{\alpha_N}(\mathbf{q}_N) \end{bmatrix} , \qquad (2.63)$$

where we defined the functions as:

$$u_{\alpha_i}(\mathbf{q}_j) \equiv u_{n,l,m_l,m_s}(\mathbf{q}_j) = u_{n,l,m_l}(\mathbf{r}_j) \chi_{\frac{1}{2},m_s} , \qquad (2.64)$$

with χ the spin function relative to the j-th electron and $u_{n,l,m_l}(\mathbf{r}_j)$ the spatial eigenfunction, both depending by their quantum numbers. From (2.63) we notice that $\psi_c(\mathbf{q}_1,..,\mathbf{q}_N)$ is antisymmetric for the exchange of any pair of electrons as requested by Pauli's principle, it vanishes when we have the same set of quantum numbers, because the determinant has linear dependent vectors, and finally the energy eigenvalue associated is the sum of the individual orbitals contributions. This discussion is valid for every element; the differences between atoms are in the type of central potential obtained and in the attractive coulombic terms. However, once we know those terms we can proceed by using variational method to find the final result of the interested quantum state. Without giving any demonstration, a good estimation of the total energy of a specific quantum state is given by:

$$E = E_u + \Delta E = E_u + \langle \Psi|H_1|\Psi\rangle , \qquad (2.65)$$

where E_u is the unperturbed energy relative to $\psi_c(\mathbf{q}_1, .., \mathbf{q}_N)$ and H_1 are the non-central terms given from equation (2.59).

2.3   Spontaneous and stimulated emission

In the previous paragraphs we have introduced the atomic orbital theory, now it's time we introduce the physics of the absorption and emission of photons, in particular *spontaneous* and *stimulated* emission.

As we know, one of the ways an atom has to exchange energy with its surrounding is by absorbing and emitting photons; when these processes occur, the atom changes its energetic state. Now, after absorbing a photon the atom has different ways to get back to its ground state, that can be either radiative or non-radiative. If we consider radiative emissions, we found that there are two possible ones: *spontaneous*, which gives rises to photoluminescence phenomena, and *stimulated* emissions, which is used to create *lasers*. Spontaneous emission occurs when an atom emits a photon without receiving any other external interactions, which cause an uniform distribution of emitted photons throughout the space. Stimulated emission is a stochastic process of quantum resonance, therefore it needs an external perturbation in order to happen; briefly, it occurs when an atom is excited by a sequence of photons that comprise an electromagnetic field applied to the atom itself[26]. The main properties of *stimulated emission* are two:

(a) The stimulated photons have the same energy as the stimulating ones and hence the same frequency.

(b) The light waves associated to the stimulated photons are in phase and have the same state of polarization of the stimulating waves.

These properties assure us that the stimulated radiation is coherent. Under normal conditions of thermal equilibrium it is extremely more likely to observe spontaneous emission, by a factor of $\sim 10^{32} : 1$; that's why most of the radiation source emits incoherent radiations.

Let's assume we have N_0 atoms in a generic ground state E_0 that transit to an excited one E_1. We indicate the absorption rate $P_{0 \to 1}$ from E_0 to E_1 with:

$$P_{0 \to 1} = N_0(nh\nu)B_{0,1} = N_0 \, \rho_\nu B_{0,1} \; , \tag{2.66}$$

where n is the number of stimulating photons per unit volume, $h\nu$ is the energy of each photon and therefore $\rho(\nu) = nh\nu$ is the energy density of the absorbed photons; $B_{0,1}$ is a constant coefficient. Analogously we repeat the argument for the stimulated emission rate:

$$P_{1 \to 0} = -N_1(nh\nu)B_{1,0} = -N_1 \, \rho_\nu B_{1,0} \; , \tag{2.67}$$

where N_1 is the number of atoms in the excited state E_1 and $B_{1,0}$ is another constant coefficient. We note that the energy density ρ_ν is the same because the required external perturbation doesn't change with time. Finally, we simply define the spontaneous emission rate $S_{1,0}$ as:

$$S_{1\rightarrow0} = N_1 A_{1,0} \ , \tag{2.68}$$

with the last constant coefficient $A_{1,0}$. These three coefficients $B_{0,1}$, $B_{1,0}$ and $A_{1,0}$ are called *Einstein coefficients*, because of Einstein's work on them[26]. It's important to notice that both $P_{0\rightarrow1}$ and $P_{1\rightarrow0}$ depend on the energy density ρ_ν, unlikely $S_{1\rightarrow0}$. It's reasonable to think the following relation between the rates must hold:

$$P_{0\rightarrow1} = P_{1\rightarrow0} + S_{1\rightarrow0} \ , \tag{2.69}$$

from which we can explicit ρ_ν as

$$\rho(\nu) = \frac{A_{1,0}/B_{1,0}}{(B_{0,1}N_0)/(B_{1,0}N_1) - 1} \ . \tag{2.70}$$

Now, we know from statistical mechanics that the number of atoms N_j in the *i-th* level of a system in thermal equilibrium conditions is given by Boltzmann distribution:

$$N_j = N_{tot} \frac{\exp\left(-E_j/k_B T\right)}{\sum_i \exp\left(-E_i/k_B T\right)} \ , \tag{2.71}$$

where N_{tot} is the total number of atoms , E_j is the energy relative to the level j and k_B is Boltzmann constant. From equation (2.71) we can easily obtain the ratio of the atoms relative to two different energy levels, in our case between N_1 and N_0, as follow:

$$\frac{N_0}{N_1} = \frac{\cancel{N_{tot}}}{\cancel{N_{tot}}} \cdot \frac{\exp\left(-E_0/k_B T\right)}{\cancel{\sum_i \exp\left(-E_i/k_B T\right)}} \cdot \frac{\cancel{\sum_i \exp\left(-E_i/k_B T\right)}}{\exp\left(-E_1/k_B T\right)} = \exp\left[(E_1 - E_0)/k_B T\right] \tag{2.72}$$

and by substituting this ratio in equation (2.70) and using *Planck-Einstein* relations we obtain:

$$\rho(\nu) = \frac{A_{1,0}/B_{1,0}}{(B_{0,1}/B_{1,0})\exp(h\nu/k_B T) - 1} \ . \tag{2.73}$$

We recall the relation of the energy density of black body radiation in thermal equilibrium

$$\rho_b(\nu) = \frac{8\pi h\nu^3}{c^3}\left(\frac{1}{\exp(h\nu/k_B T) - 1}\right) \ , \tag{2.74}$$

which must be consistent with the one expressed by relation (2.73), hence we conclude that[26]:

$$\frac{B_{0,1}}{B_{1,0}} = 1 \ , \tag{2.75}$$

$$\frac{A_{1,0}}{B_{1,0}} = \frac{8\pi h\nu^3}{c^3} \ . \tag{2.76}$$

These relations were first obtained by Einstein (1879-1955) in 1917. The value of the coefficients is unknown and depends on the atoms and the energy levels we consider. It's important to highlight that from (2.76) we see how the energy difference between the two levels affects the probability of having spontaneous or stimulated emission by a factor of ν^3 .

Chapter 3

Presentation of the project

In the first chapter we have seen some curious luminous phenomena, in particular phosphorescence and fluorescence, which has been studied and observed since the XVI century; recently these phenomena has been better understood and they have been used in a wide variety of ways, from entertainment to scientific applications. After this first introduction to the topic, we have analyzed the basics behind luminous phenomena, especially the way the matter interact with electromagnetic radiation from a semi-classical and quantum point of view, giving particular importance to the atomic model and how it is structured.

The purpose of this final chapter is to present a simple idea of how we can generate and control luminous phenomena in order to replicate images or scenes, utilizing when it's required the theory previously made. We'll begin by presenting the ideal situation of the apparatus, then we will tackle the problem analytically with some approximations and finally we'll draw some conclusions on the possibility of creating the phenomenon requested.

As well as the other luminous gadgets created, a more efficient version of this project could be used both in entertainment and science field; we can imagine it utilized for example as a 3D real-time representation of a human organ, or a 3D function visualizer.

3.1 Description of the model

The result we want to obtain is simple: illuminate a small portion of space and being able to accurately move it in a free space. If we manage to come up a device who's capable of satisfy the requested condition, we can utilize the *afterimage* of the point to generate more complex figures by moving it quickly in a portion of space. Now, obviously it's impossible to represent full images with just a point; fortunately the human eye isn't capable of distinguish more than 30Hz of image refresh on average. In addition, the illusion of a moving scene can be obtained even with a refresh rate of 15Hz.

The idea of the model is the following: we utilize a monoatomic gas contained in a finite volume and exploit its excitation properties in order to obtained localized transitions that emit visible light; we use fast laser impulses to excite the atom where required. The main requirements are:

(a) The emission of visible light must be isotropic, so it must be equally distributed on a solid angle.

(b) The laser light used to excite the atoms must be out of the visible spectrum, so that scatter effects won't be noticed.

(c) The transition rate must be fast, possibly a lot more then the human eye refresh rate. Also, faster transition rates allow us to move the point faster around the space, so that we can create bigger images with the same dot.

(d) The intensity of the visible emission must be enough to be perceived, possibly even in medium light conditions.

It's important to notice that the points above are just a heavy restriction of the pool of elements that we can choose from; the study we have done it was based on the *rubidium* (Rb) in gas state, mainly because it gives the possibility to satisfy the point (b), and because it is a monoatomic gas. There's nothing holding us on this particular element; if there are better compounds, or easier elements to handle, we're more than happy to use them. However, the following discussion is general enough to be applied on every monoatomic gas.

3.1.1 Energetic levels and transitions

Let's consider a limited volume V filled by N_{tot} atoms of the same element Z. We reasonably assume that all the atoms are at first in the ground state ε_0 and are maintained at thermal equilibrium at a temperature T. Let assume that the motion of the atoms is slow enough to ignore relativistic effects; this request has to be analyzed buy estimating

the velocity of atoms in that volume. Using Maxwell speed distribution, we obtain:

$$\bar{v}_Z = \sqrt{\frac{3k_B T}{m_Z}} \ , \tag{3.1}$$

where k_B is Boltzmann constant and m_Z is the mass of an atom Z. We ask that $\bar{v}_Z \ll c$, in particular that $\bar{v}_Z$ is less than 5% of the speed of light ($\sim 1.5 \cdot 10^7 m/s$). We find that:

$$T_{max} = \frac{m_Z c^2}{1200 k_B} \ , \tag{3.2}$$

and that all the temperature values must lay under that limit. This is obviously respected for almost every laboratory situation we can imagine, but soon we will see that we have to add another restriction to the temperature. In fact, we should request that all the atoms that are first excited by the first laser will remain in the volume V_{eff} until the second one arrives. If the distance between L_2 and the volume is d_p, then the time required from the laser impulse to get there will be:

$$t_d = \frac{d_p}{c} \ . \tag{3.3}$$

Let d_{eff} be the linear dimensions of the volume V_eff; we impose that the distance traveled by one atom in the volume in a time t_d has to be less than the volume linear dimensions:

$$\bar{v}_Z \, t_d < d_{eff} \ , \tag{3.4}$$

which gives us the following condition on the temperature:

$$T'_{max} = \frac{d_{eff}^2 \, c^2 \, m_Z}{3 \, d_p^2 \, k_B} \ . \tag{3.5}$$

Figure 3.1: Representation of the transitions required for the atom Z. It first goes to the level ε_1, then to ε_2 and finally it goes back to the ground state.

If the first laser is constant, this condition can be reasonably ignored. Now let's take one of the atoms available and we consider three of it's energy levels where relations (2.57) hold: ε_0 the ground state, ε_1 and ε_2 the excited ones, with $\varepsilon_2 > \varepsilon_1$. The transitions that we want are shown in Figure 3.1. In order to have those transitions we have to use two different lasers, one for each upper jump; the two lasers L_1 and L_2 will have wavelength λ_1 and λ_2 which are relative to the jumps $\varepsilon_0 \rightarrow \varepsilon_1$ and $\varepsilon_1 \rightarrow \varepsilon_2$ respectively. As requested by point (b), both the wavelength are out of the visible spectrum. The transition that we are interested in is the spontaneous one from

the intermediate energy level $\overline{\varepsilon}$ to the ground $\overline{\varepsilon} \to \varepsilon_0$; as we know from Planck-Einstein relations, the wavelength of the photon emitted in that transition is:

$$\overline{\lambda} = \frac{c\,h}{\Delta E} = \frac{c\,h}{\overline{\varepsilon} - \varepsilon_0} \ , \tag{3.6}$$

this wavelength must be in the visible spectrum, so we have the following restriction: $\overline{\lambda} \in [400\,\mathrm{nm}, 700\,\mathrm{nm}]$. It also has been measured that the maximum spectral sensitivity of the human eye under daylight conditions is at a wavelength of 555 nm, while at night the peak shifts to 507 nm[32]. This information suggests us that if we want the to increase the efficiency of the device, it could be useful to study carefully some elements who have this wavelength emission as the one used to realize the image. The rubidium (Rb) transition utilize in our study has a wavelength emission of 420 nm. Now that we have established the transition pattern we want to replicate, we need to maximize the number of atoms that will decay from ε_2 to ε_0.

3.1.2   Two laser interaction volume

First of all, let's consider the spatial dimensions of the point that we will use to draw our image; it will be the result of the intersection between two laser beams, which we assume to be cylindrical and with the same radius $r_1 = r_2 = r$. The intersection can be calculated with a multiple integral, which gives the following result:

$$V_{eff} = \frac{8}{3}r^3(\tan(\theta/2) + \cot(\theta/2)) = \frac{8}{3}r^3\left(\frac{2}{\sin\theta}\right) \ , \tag{3.7}$$

where θ is the angle between the direction of the two beams; the footnote "eff" means "effective", because it gives the actual maximum of atoms we can use in our process. In fact, from the N_{tot} atoms we have in our volume V now we just consider a very small portion of it, which is indeed V_{eff}. It's clear that the equation (3.7) is useful only if the two beams are not parallel, since the volume would be infinite; in order to avoid that singularity we could define some boundary conditions, but it's not of primary interest here, because the angle θ is always contained in a rage of approximately 25° to 55°. We can now estimate the number of atom that we can use as a simple ratio between the effective volume and the total one:

$$N_{eff} = N_{tot} \cdot \frac{V_{eff}}{V} \ , \tag{3.8}$$

as long as we can consider the atoms equally distributed in the whole volume. Another easy way to estimate the volume of the intersection is by using *Monte Carlo method*, by simulating the probability of a point being outside the intersection; an example is shown in Figure 3.2, with the code in *Appendix B*.

Cylinder Intersection
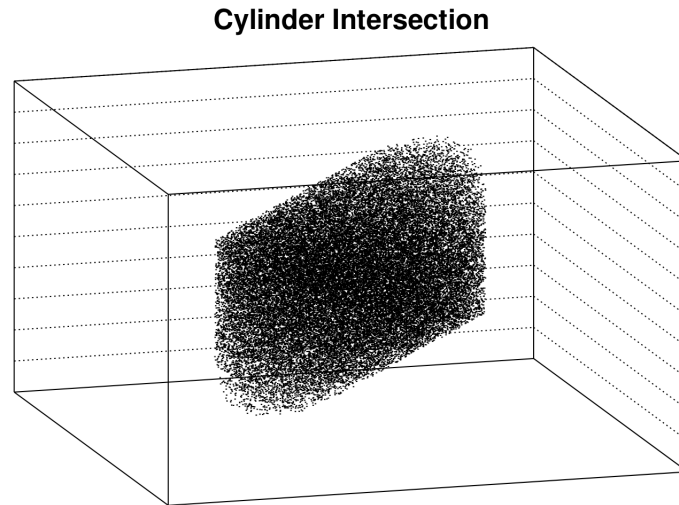
Figure 3.2: 3D simulation of the points contained in the intersection of two cylinders with *Monte Carlo method.*

3.1.3 The excitation process

Now we can consider the excitation processes; as we have seen in the previous chapter, in order to excite an atom from a level A to another B it has to interact with a photon with an energy equal to the energy gap between the two levels. This will affect the number of photons in V_{eff} coming from the two beams; in fact, the one with wavelength λ_1 will interact with all the atoms on its way to V_{eff}, while the other beam won't because of its different wavelength λ_2. This factor has to be taken into account when choosing the power of the two lasers, especially if the distance traveled from the first beam is fairly large. Let's consider the N_{eff} atoms: if we made interact these atoms with L_1 constant, what we would get would be a good number of excited atoms N_1 in ε_1, but even the possibility of a stimulated emission described by equation (2.67) that we would like to avoid.

Now, it's impossible to completely remove the stimulated emissions, however we can limit them by using laser pulses of a specific duration. The duration of the beams can be estimated knowing the average life time of the excited levels; let's consider ε_i and ε_{i+1} first: it's clear that with the beam L_i constant the number $N_i = N_i(t)$ of excited atoms will get to a maximum value such that:

$$N_i(t = t_{max}) < N_{eff} . \tag{3.9}$$

What's important is that we don't have to keep the laser on to get to that value; in fact, after the excitation of the first atom, the number $N_i(t)$ grows approximately unperturbed

for all the duration of the level average life time, that we name $t = \tau_i$. We call the maximum number of atoms in the excited energy level ε_i as $\overline{N}_i = \overline{N}_i(\rho(\lambda_i))$, where $\rho(\lambda_i)$ is the energy density of the absorbed photons relative to the laser L_i. The dependence from the energy of the beam is clear, since more energy implies more photons; however, from the theory of Einstein coefficients, we see that the number of atoms that can be excited will be at most $1/2$ of the total as shown in equation (2.75). In addition, since the laser pulse is a quick external interaction force, the *Breit-Wigner distribution* allows us to calculate the resonance frequencies that we want to use in order to have the maximum excitation:

$$I(\omega) = \frac{k}{(\omega - \omega_0)^2 + \frac{\Gamma^2}{4}} \ , \tag{3.10}$$

where ω_0 is the mean energetic value of the level, k is a physical constant, Γ is the energy level width, which it's related to the average lifetime by the relation:

$$\Gamma = \frac{\hbar}{\tau} \ . \tag{3.11}$$

Equation (3.10) gives us the best laser width that it needs to have; in fact, as it happens in classical mechanics, if the laser *Breit-Wigner distribution* is the same of the distribution of the level we will have an intense resonance phenomenon. Besides, if the laser width is too large it could alter the image by exciting other energy levels. We conclude that the duration of the laser process has to be equal to the average lifetime of the excited level plus eventually some correction terms that depends on the amount of photons lost during the path:

$$t_i = \tau_i + t'_i \ ; \tag{3.12}$$

This discussion is valid for both the excitation steps. Now, the idea of having pulsed laser came form the necessity to minimize the stimulated emission; however, if we consider the level ε_1, its population after the ending of the perturbation will decrees exponentially; this results in a significant loss of excited atoms. We could increase the duration of the pulse, but at that point we will have stimulated emissions anyway. Some more accurate estimates could be done in the future; by now, we will consider the first laser L_1 constant, so that to a first approximation we will have a constant number of atoms in the level ε_1. The second laser L_2 will remain pulsed, since the time that the atoms spend in the level ε_2 is irrelevant.

Assuming that L_2 last for a time $t_2 = \tau_2$ we finally managed to get the maximum number of atoms $\overline{N}_2(\rho(\lambda_2))$ in the final excited level, so that we can proceed with the last part of the process. As we see in Figure 3.1, we impose that between the levels ε_2 and ε_0 there is at least another level $\bar{\varepsilon}$ additional to ε_1 such that the transition $\varepsilon_2 \to \bar{\varepsilon}$ is permitted, while the one $\varepsilon_2 \to \varepsilon_0$ is forbidden by the selection rules. The atoms that will perform the spontaneous transition $\varepsilon_2 \to \bar{\varepsilon}$ will be a portion of $\overline{N}_2(\rho(\lambda_2))$; in fact, the probability of following one decay path instead of the other depends on the *energy gap* between the

levels and their widths. It's inevitable that a relevant fraction of atoms will decay back to the level ε_1; however, having L_1 constant helps in regaining some of the atoms according to (2.66). Then it occurs the spontaneous transitions $\bar{\varepsilon} \to \varepsilon_0$ that we are interested in, which gives the number of photons $N_\gamma = \overline{N}$ distributed on the solid angle. Basically, the goal of the study is to to maximize the number of atoms $\overline{N}$ on the energy level $\bar{\varepsilon}$.

In order to simplify the problem, we define the laser impulse as the following function:

$$\rho_\nu(t) = \begin{cases} \xi, & 0 < t \le t_{max} \\ 0, & t > t_{max} . \end{cases} \tag{3.13}$$

Let's consider the very first transition; The differential equation describing the level population by using a pulsed laser is:

$$\frac{dN_0(t)}{dt} = -N_0(t)\rho_\nu(t)B_{0,1} + N_1(t)A_{1,0} + N_1(t)\rho_\nu(t)B_{1,0} + \overline{N}(t)A_{\bar{\varepsilon},0} . \tag{3.14}$$

This is a linear differential equation with non constant coefficients that is not easy to elaborate, even with the impulse simplification. Using a constant laser instead, we can extremely simplify this first step considering just the mean value of atoms N_0 after a certain amount of time; this allows us to treat the level of the population $N_1(t) = N_{eff} - N_0$ as constant. With this said, we can consider the second transition, which is described by the equation:

$$\frac{dN_2(t)}{dt} = N_1\rho_\nu(t)B_{1,2} - N_2(t)\Gamma_2 - N_2(t)\rho_\nu(t)B_{2,1} . \tag{3.15}$$

If we eliminate the last term, we can rewrite the differential equation:

$$\frac{dN_2(t)}{dt} + N_2(t)\Gamma_2 = N_1\rho_\nu(t)B_{1,2} = N_1 B_{1,2} \cdot \begin{cases} \xi, & 0 < t \le t_{max} \\ 0, & t > t_{max} , \end{cases} \tag{3.16}$$

which gives the following solution:

$$N_2(t) = \begin{cases} N_1 B_{1,2}\,\xi(1 - e^{-\Gamma_2 t}), & 0 < t \le t_{max} \\ N_2'\,e^{-\Gamma_2 t}, & t > t_{max} , \end{cases} \tag{3.17}$$

where we have used the boundary conditions $N_2(0) = 0$ and $N_2(+\infty) = 0$, with the coefficient N_2' representing the maximum number of excited atoms in the energy level ε_2:

$$N_2' = N_1 B_{1,2}\,\xi(e^{\Gamma_2 t_{max}} - 1) . \tag{3.18}$$

The relation (3.18) can be obtained by imposing the continuity of the function $N_2(t)$ for $t = t_{max}$; we can see the plot of the function obtained in Figure 3.3. This discussion
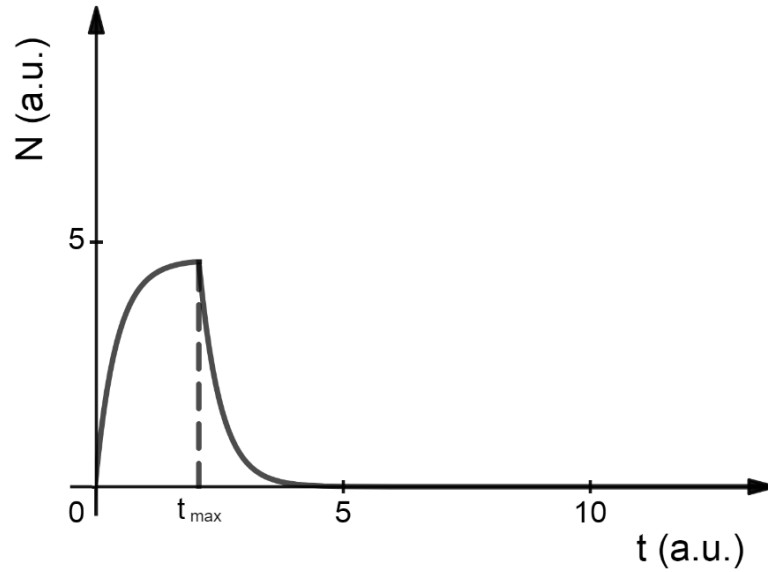
Figure 3.3: Plot of the function $N_2(t)$ according to the solution found of the differential equation.

is strictly connected with the rubidium transitions studied, but it's not mandatory to follow the same pattern for other possible elements.

Now that we have the number of atoms in the final excited level, we can find the number N_γ of photons emitted from the transition $\bar{\varepsilon} \rightarrow \varepsilon_0$ by knowing the interested decay probability $\overline{P_2}$:

$$N_\gamma = N_2(t)\,\overline{P_2}\ . \tag{3.19}$$

We show now a rough first estimates of the number of photons equally distributed on the solid angle, considering the best case scenario. Let's start with N_{eff} atoms; we lose half atoms in the transition $\varepsilon_0 \rightarrow \varepsilon_1$. After that, assuming that the laser L_2 is pulsed, the number of atoms on the level ε_2 will be N_2' at most, which depends from N_1.

Finally, we can obtain the number of atoms that decay to the level $\bar{\varepsilon}$, by the simple relation: $N_2'\,\overline{P_2}$. The pattern of the transitions with the associated probabilities is outlined in Figure 3.4. This leads to the relation:

$$N_\gamma = \frac{N_{eff}}{2}\,\overline{P_2}\,B_{1,2}\,\xi(e^{\Gamma_2 t_{max}} - 1)\ . \tag{3.20}$$

It's clear that just a small portion of that number will be perceived form the eye, which will be proportional to the vision solid angle. Then, that portion needs to be compared with the minimum intensity required from the human eye in order to see the luminous point. If that value is below the minimum required some changes has to be made to the device, which could be increasing the number of atoms N_{tot}, changing the element Z, or even using a special camera that allows the perception of even a small amount
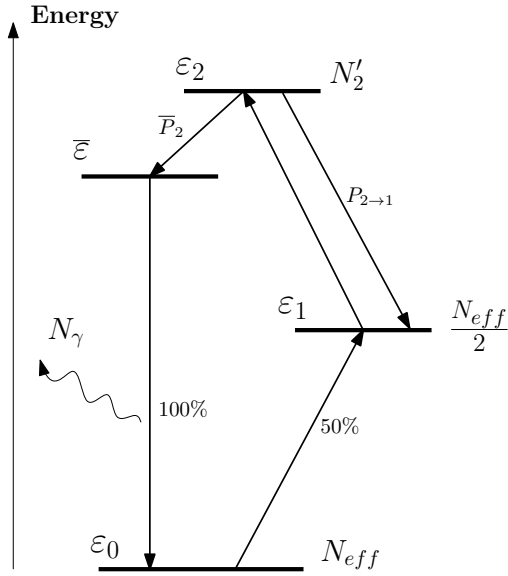
Figure 3.4: Simple schematization of the absorption/emission processes considering all the approximations.

of photons. Once the luminous point is obtained, we can move it around and create afterimages; in order to represent more complex figures we can divide the whole volume in sub-volumes, each with its luminous point operating.

3.2 Expected light yield

The two laser excitation process proposed required that the one relative to the first transition is constant, while the second one is pulsed. The total number of effective atoms that can perform the transitions are obtained by the intersection of the two lasers, which is:

$$N_{eff} = N_{tot} \cdot \frac{8}{3V} r^3 \left(\frac{2}{\sin \theta} \right) , \tag{3.21}$$

where N_{tot} are the atoms contained in the whole volume V, assuming that the ray of the two lasers is the same. After a series of assumptions and approximations, we managed to obtained a rough estimation of the total number of photons emitted for the transition considered through the whole solid angle. This number is given by the following expression:

$$N_{\gamma} = \frac{N_{eff}}{2} \overline{P_2} B_{1,2} \xi (e^{\Gamma_2 t_{max}} - 1) .$$

Now, the photons that are actually perceived by the human eye are just a small fraction of N_{γ}; this fraction will be proportional to the field of view of the eye. Then, depending

upon the environment light conditions, the intensity required of the emission will be higher or lower; in a dark room will be way easier to perceive the phenomenon instead of a bright one.

3.3　An example: transitions in a rubidium atom

There are several hydrogenoid atoms that can be used as concrete examples; due to the wide literature available we consider a rubidium atom. The transitions that satisfy the conditions required are shown in Figure 3.5. We can see the correspondence between the levels used in the mathematical model and the ones that are used to excite the rubidium atom:

$$\begin{cases} \varepsilon_0 \longrightarrow 5S_{1/2} \\ \varepsilon_1 \longrightarrow 5P_{3/2} \\ \varepsilon_2 \longrightarrow 5D_{5/2} \\ \overline{\varepsilon} \longrightarrow 6S_{3/2} \ , \end{cases}$$

where $5S_{1/2}$ is in fact the rubidium ground state. In addition, we see that the energy gaps between the levels are exactly the ones we need in order to have a spontaneous emission of "visible" photons as the result of a double excitation by two infrared lasers. The two lasers wavelength required to excite the rubidium are:

$$\begin{cases} \lambda_1 = 780\text{nm} \\ \lambda_2 = 776\text{nm} \ ; \end{cases}$$

we see now why we want the lasers to have a narrow width; the laser must excite only the level their supposed to, or the image could be corrupted. Finally, we see that the emitted photon wavelength is $\overline{\lambda} = 420\text{nm}$, which is relative to a bluish color and with an energy of:

$$\Delta E = \frac{c\,h}{\overline{\lambda}} = 2.95\,\text{eV} \ . \tag{3.22}$$

That's a good example of an element that satisfy the strict parameters we imposed for our study. The problems will now just be technical ones, the possibility of generating luminous points in space is guaranteed by the theory and the experimental values[33].
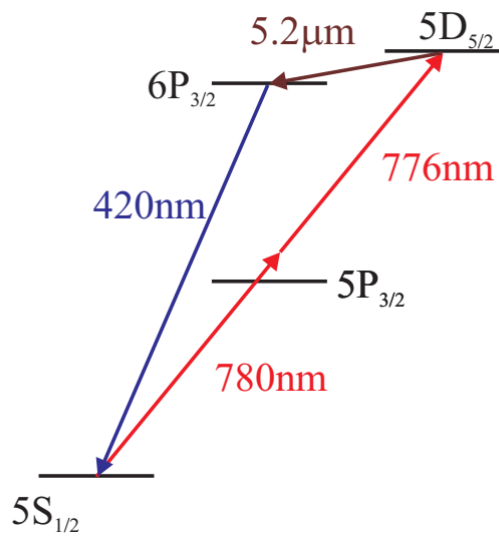
Figure 3.5: Transitions pattern for rubidium atom that generate visible radiation from two infrared lasers. As we can see, the wavelength of the photons emitted is $\overline{\lambda} = 420$nm, that corresponds to a blue light.

Conclusions

The aim of this thesis was to find a method to generate luminous images in space. We wanted to generate a luminous point in space and being able to move it freely in a limited volume. The solution was found in the process of stimulated emission; in particular, it has been used a four-level energy system with a precise transition pattern that must be performed. The four-level model is suggested by the opportunity to have a spontaneous emission of photons with frequency in the visible spectrum as the result.

In order to describe the system, we have studied the atomic structure of atoms and how it improved until the fine structure. We have analyzed the mechanisms involved in atomic transitions so that we could understand how the system evolved after an excitation or a de-excitation. We also wanted to know the behavior of the energy level populations after the interaction with the external photons, therefore we introduced *Einstein coefficients*. Our work has begun with the estimations of the total atoms that could be used for our purpose, then we manage to set a mathematical model that described the system. After some necessary approxmations, the mathematical model we chose allowed us to obtain the maximum value of photons spontaneously emitted, which is given by the following expression:

$$N_\gamma = \frac{N_{eff}}{2} \, \overline{P_2} \, B_{1,2} \, \xi(e^{\Gamma_2 t_{max}} - 1) \ .$$

At the end of the study we were able to obtain a physical model capable of describing the transition pattern proposed, which gives us the theoretical possibility of generating "visible" light by using two "non-visible" laser beams.

This pattern is also realistically doable; in fact, we have found an element (rubidium) who follows the exact same transitions required and that perfectly matches the requested values for the wavelengths relatives to the emission/absorption processes. The ideas explored here need to be verified experimentally; a crucial help to the model could be obtained by collecting and analyzing experimental data, only part of them are known from literature. Notwithstanding the limitations of this first approach to the problem of generating holograms in space by point-light sources, we've found a viable solution that is worth to be studied further.

Appendix A: Table of physical constants

Name	Symbol	Value	Unit
Elementary charge	e	$1.60217733 \cdot 10^{-19}$	C
Fine-structure constant	$\alpha = e^2/(2hc\varepsilon_0)$	$\approx 1/137$	
Speed of light in vacuum	c	$2.99792458 \cdot 10^8$	m/s (def)
Permittivity of the vacuum	ε_0	$8.854187 \cdot 10^{-12}$	F/m
Permeability of the vacuum	μ_0	$4\pi \cdot 10^{-7}$	H/m
$(4\pi\varepsilon_0)^{-1}$		$8.9876 \cdot 10^9$	$\mathrm{Nm^2C^{-2}}$
Planck's constant	h	$6.6260755 \cdot 10^{-34}$	Js
Reduced Planck constant	$\hbar = h/2\pi$	$1.0545727 \cdot 10^{-34}$	Js
Bohr magneton	$\mu_b = e\hbar/2m_e$	$9.2741 \cdot 10^{-24}$	$\mathrm{Am^2}$
Bohr radius	a_0	52.918	pm
Rydberg's constant	Ry	13.595	eV
Electron Compton wavelength	$\lambda_{Ce} = h/m_e c$	$2.2463 \cdot 10^{-12}$	m
Proton Compton wavelength	$\lambda_{Cp} = h/m_p c$	$1.3214 \cdot 10^{-15}$	m
Reduced mass of the H-atom	μ_H	$9.1045755 \cdot 10^{-31}$	kg
Rydberg constant of hydrogen	R_H	10967757.6	$\mathrm{m^{-1}}$
Stefan-Boltzmann's constant	σ	$5.67032 \cdot 10^{-8}$	$\mathrm{Wm^{-2}K^{-4}}$
Wien's constant	k_W	$2.8978 \cdot 10^{-3}$	mK
Molar gasconstant	R	8.31441	$\mathrm{J \cdot mol^{-1} \cdot K^{-1}}$
Avogadro's constant	N_A	$6.0221367 \cdot 10^{23}$	$\mathrm{mol^{-1}}$
Boltzmann's constant	$k_B = R/N_A$	$1.380658 \cdot 10^{-23}$	J/K
Electron mass	m_e	$9.1093897 \cdot 10^{-31}$	kg
Proton mass	m_p	$1.6726231 \cdot 10^{-27}$	kg
Neutron mass	m_n	$1.674954 \cdot 10^{-27}$	kg
Elementary mass unit	$m_u = \frac{1}{12}m\left(^{12}_{6}\mathrm{C}\right)$	$1.6605656 \cdot 10^{-27}$	kg
Nuclear magneton	μ_N	$5.0508 \cdot 10^{-27}$	J/T
Atomic Units	**Symbol**	**Value**	**Unit**
Electron mass	m_e	1	a.u.
Elementary charge	e	1	a.u.
Reduced Planck constant	$\hbar$	1	a.u.
Permittivity of the vacuum	$4\pi\varepsilon_0$	1	a.u.
Boltzmann's constant	k_B	1	a.u.

Appendix B: ROOT program for laser intersection volume

```cpp
#include <iostream>
#include<cstdlib>
#include<cmath>
#include<random>
#include<ctime>
#include<TGraph2D.h>
#include<TCanvas.h>
#include<TPad.h>
#include<TRandom.h>

//*----------------------------------------------------------*

//In order to run this program you have to install ROOT CERN.

//*----------------------------------------------------------*

double MIN = -10000, MAX = 10000; //Box dimension respect to the origin.
int INSIDE = 0, OUTSIDE = 0, POINTS=100000, PRIMO=0,SECONDO=0;

const double RADIUS = 5000;

double cylinderVersor1[3] = { sqrt(2./3.), 1./sqrt(6.), 1./sqrt(6.) };
//double cylinderVersor1[3] = { 1. / sqrt(3.), 1. / sqrt(3.) , 1. /
sqrt(3.) };
//double cylinderVersor1[3] = { sqrt(3.)/2.,1./2.,0.};
double cylinderVersor2[3] = { 0.,0.,1. };

double pointVector[3];
double *vectorProjection1 = new double[3];
double *vectorProjection2 = new double[3];

TGraph2D *Space=new TGraph2D(POINTS);
TGraph2D *firstCylinder=new TGraph2D(POINTS);
TGraph2D *secondCylinder=new TGraph2D(POINTS);

TRandom R=TRandom();

TGraph2D *box=new TGraph2D(POINTS);
//TGraph2D *zulu=new TGraph2D(POINTS);

std::default_random_engine generator{static_cast<long unsigned
int>(time(0)) };
std::uniform_int_distribution<int> Uniform(MIN, MAX);

double Norm(double *v1)
{
    return sqrt(v1[0] * v1[0] + v1[1] * v1[1] + v1[2] * v1[2]);
}

double* VectorialDifference(double *v1, double *v2)
{
    double *v3 = new double[3];
    v3[0] = v1[0] - v2[0];
    v3[1] = v1[1] - v2[1];
```

```
      v3[2] = v1[2] - v2[2];
      return v3;
}

double ScalarProduct(double* v1, double* versor)
{
      return (v1[0] * versor[0] + v1[1] * versor[1] + v1[2] * versor[2]);
}

int main()
{
      for (int i = 0; i < POINTS; i++)
      {
                  pointVector[0] = Uniform(generator);
                  pointVector[1] = Uniform(generator);
                  pointVector[2] = Uniform(generator);

                  box-
>SetPoint(i,pointVector[0],pointVector[1],pointVector[2]);

                  vectorProjection1[0] = cylinderVersor1[0] *
ScalarProduct(pointVector, cylinderVersor1);
                  vectorProjection1[1] = cylinderVersor1[1] *
ScalarProduct(pointVector, cylinderVersor1);
                  vectorProjection1[2] = cylinderVersor1[2] *
ScalarProduct(pointVector, cylinderVersor1);

                  vectorProjection2[0] = cylinderVersor2[0] *
ScalarProduct(pointVector, cylinderVersor2);
                  vectorProjection2[1] = cylinderVersor2[1] *
ScalarProduct(pointVector, cylinderVersor2);
                  vectorProjection2[2] = cylinderVersor2[2] *
ScalarProduct(pointVector, cylinderVersor2);

                  //std::cout<<"Componenti Punto:
("<<pointVector[0]<<','<<pointVector[1]<<','<<pointVector[2]<<")\n\n";
                  //std::cout<<"Risultato Differenza (<5000 NECESSARIO):
("<<Norm(VectorialDifference(pointVector, vectorProjection1))<<")\n\n";

                  if(Norm(VectorialDifference(pointVector,
vectorProjection1)) <= RADIUS)
                  {PRIMO=PRIMO+1;
                  //std::cout<<"Componenti Punto (PRESO):
("<<pointVector[0]<<','<<pointVector[1]<<','<<pointVector[2]<<")\n\n";
                  firstCylinder-
>SetPoint(i,pointVector[0],pointVector[1],pointVector[2]);
                  }
                  if(Norm(VectorialDifference(pointVector,
vectorProjection2)) <= RADIUS)
                  {SECONDO=SECONDO+1;
                  secondCylinder-
>SetPoint(SECONDO,pointVector[0],pointVector[1],pointVector[2]);
                  }
```

```
                  if (Norm(VectorialDifference(pointVector,
vectorProjection1)) <= RADIUS &&
                        Norm(VectorialDifference(pointVector,
vectorProjection2)) <= RADIUS)
                  {
                        Space-
>SetPoint(INSIDE,pointVector[0],pointVector[1],pointVector[2]);
                        INSIDE = INSIDE + 1;
                  }
                  else OUTSIDE = OUTSIDE + 1;
      }

      TCanvas *Box=new TCanvas("Box","Box");
      //box->SetMargin(0.5);
      box->SetTitle("Box");
      box->SetMarkerColor(2);
      box->Draw("P");

      TCanvas *cylinderIntersection=new
TCanvas("cylinderIntersection","Cylinder Intersection");
      Space->GetXaxis()->SetRange(2*MAX);
      Space->SetMarkerColor(kBlack);
      Space->SetTitle("Cylinder Intersection");
      Space->Draw("P R");

      TCanvas *cylinder1=new TCanvas("cylinder1","First Cylinder");
      //firstCylinder->SetMargin(0.5);
      firstCylinder->SetMarkerColor(kRed);
      firstCylinder->SetTitle("First Cylinder");
      firstCylinder->Draw("P");

      TCanvas *cylinder2=new TCanvas("cylinder2","Second Cylinder");
      secondCylinder->SetMargin(0.5);
      secondCylinder->SetMarkerColor(kRed);
      secondCylinder->SetTitle("Second Cylinder");
      secondCylinder->Draw("P");

      std::cout << " -Points Inside: " << INSIDE << std::endl;
      std::cout << " -Points Outside: " << OUTSIDE << std::endl;
      std::cout << " -Volume Fraction: " << INSIDE / (double)(INSIDE +
OUTSIDE) << std::endl;
}
```

Bibliography

[1] S. E. Braslavsky. *Glossary of terms used in Photochemistry, 3rd Edition.* Pure Appl. Chem., Vol. 79, No. 3, pp. 293–465, 2007.

[2] J. I. Zink, B. P. Chandra. *Light emission during growth and destruction of crystals. Crystalloluminescence and triboluminescence.* Journal of Physical Chemistry, Vol. 86, No. 1, pp. 5-7, 1982.

[3] B Valeur, J. C. Brochon. *New Trends in Fluorescence Spectroscopy Applications to Chemical and Life Sciences.* Springer Publishing, 2001.

[4] B. Valeur, M. B. Santos. *A Brief History of Fluorescence and Phosphorescence before the Emergence of Quantum Theory.* Chemical Education, ,Vol. 88, pp. 731–738, 2011.

[5] G. G. Stokes. *On the Change of Refrangibility of Light.* Philosophical Transactions of the Royal Society of London. 142, 463–562, 1852.

[6] J. B. Perrin. *Atomes et lumiere.* Revue du Mois, Vol. 21, pp. 113 -166, 1920.

[7] J. B. Perrin. *Observations sur la fluorescence.* Comptes Rendus Vol. 177, pp. 469-475, 1923.

[8] F. Perrin. *Loi de decroissance du pouvoir fluorescent en fonction de la concentration.* Comptes Rendus Vol. 178, pp. 1978-1980, 1924.

[9] F. Perrin. *Fluorescence. Duree elementaire d'emission lumineuse.* Éditions Hermann, Paris, 1931.

[10] B. Nickel. EPA Newsletter Vol. 61, pp. 27-60, 1997.

[11] J. Wlodarczyk, B. Kierdaszuk. *Interpretation of Fluorescence Decays Using a Power-like Model.* Biophysical Journal, Vol. 85, pp. 589-598, 2003.

[12] D. S. Elson, L. Marcu, P. French. *Fluorescence Lifetime Spectroscopy and Imaging.* CRC Press, 2014.

[13] Comunity based. https://www.naturesrainbows.com/

[14] M. P. Anesh, S. K. H. Gulrez, A. Anis, H. Shaikh, M. E. A. Mohsin, S. M. Al-Zahrani. *Developments in Eu^{+2} - Doped Strontium Aluminate and Polymer/Strontium Aluminate Composite.* Advances in Polymer Technology, 2014.

[15] H. Yamamoto, T. Matsuzawa. *Mechanism of long phosphorescence of $SrA1_2O_4$, : Eu^{2+}, Dy^{3+} and $CaAl_2O_4$: Eu^{2+}, Dy^{3+}.* Journal of Luminescence, Vol. 72-74, pp. 287-289, 1997.

[16] *Tom Bacher Goes for the Glow*, http://theangle.whotels.com/ , 2016.

[17] G. Weber. *Uses of Fluorescence in Biophysics - Some Recent Developments.* Annual Review of Biophysics and Bioengineering, Vol. 1.1, pp. 553-570, 1972.

[18] S. A. Weinreis, J. P. Ellis, S. Cavagnero *Dynamic Fluorescence Depolarization: A Powerful Tool to Explore Protein Folding on the Ribosome.* United States National Library of Medicine, PubMed Central, 2010.

[19] R. Jenkins. *X-ray Fluorescence Spectromerty.* 2nd ed., John Wiley & Sons, 1999.

[20] Saxby, Graham. *Pratical Holography.* 3rd ed. , Institute of Physics Publishing, 2003.

[21] Gabor, Dennis. *A New Microscopic Principle.* Nature Vol. 161, pp. 777–778, 1948.

[22] *What is a fogging device?.* BBC News. 8 June 2009.

[23] http://www.biglab.co.uk/projects/mistable.

[24] R. Goldstone, P. Rutherford. *Introduction to plasma physics.* Institute of Physics Publishing, 1995.

[25] Y. Ochiai, K. Kumagai, T. Hoshi, J. Rekimoto, S. Hasegawa, Y. Hayasaki. *Fairy Lights in Femtoseconds: Aerial and Volumetric Graphics Rendered by Focused Femtosecond Laser Combined with Computational Holographic Fields.* University of Tsukuba, 2016.

[26] R. Eisberg, R. Resnick. *Quantum Physics of Atoms, Molecules, Solids, Nuclei and Particles.* 2nd ed., John Wiley & Sons, 1985.

[27] B. H. Bransden, C. J. Joachain. *Physics of atoms and molecules.* Longman Scientific & Technical, 1983.

[28] D. J. Griffiths, D. F. Schroeter. *Introduction to Quantum Mechanics.* 3rd ed. , Cambridge University Press, 2018.

[29] A. Messiah. *Quantum Mechanics.* Dover edition, two volumes in one, Dover Publications Inc., 2014.

[30] N. Bohr. *Rydberg's discovery of the spectral laws.* C.W.K. Gleerup, 1954.

[31] W. Pauli. *Exclusion principle and quantum mechanics*, Nobel Lecture, 1946.

[32] H. Gross, W. Singer, M. Totzeck. *Handbook of Optical Systems [electronic Resource]: Physical Image Formation*

[33] A. Vernier, S. Franke-Arnold, E. Riis, A. S. Arnold. *Enhanced frequency up-conversion in Rb vapor*, Optical Society of America, 2018.